

# Finite – $T$ topological Susceptibility with heavy Quarks

---

**Bruno Högl, Guy D. Moore**

*Institut für Kernphysik, Technische Universität Darmstadt  
Schlossgartenstraße 2, D-64289 Darmstadt, Germany*

*E-mail:*

[bhoegl@theorie.i kp.physik.tu-darmstadt.de](mailto:bhoegl@theorie.i kp.physik.tu-darmstadt.de), [guy.moore@physik.tu-darmstadt.de](mailto:guy.moore@physik.tu-darmstadt.de)

**ABSTRACT:** Axion cosmology needs the QCD topological susceptibility between 400 and 1100 MeV. In this range the bottom quark is inconvenient to include in lattice simulations, but not heavy enough to ignore. We estimate its effect on the susceptibility by computing the ratio of the 4-quark susceptibility and the 4+1-quark susceptibility in the caloron gas approximation. We do so by computing small-mass and large-mass expansions of the finite-mass and -temperature fluctuation determinant and connecting them with a Padé approximant.

**KEYWORDS:** Quark-Gluon Plasma, QCD, topology, caloron, bottom quark

---

## Contents

<b>1</b>	<b>Introduction and main Result</b>	<b>1</b>
<b>2</b>	<b>Preliminaries</b>	<b>4</b>
<b>3</b>	<b>Strategy of our Approach</b>	<b>9</b>
<b>4</b>	<b>Small Mass – Taylor Expansion</b>	<b>12</b>
4.1	Structure of the Expansion	12
4.2	Massless closed loop scalar Propagator	14
4.3	Taylor Expansion – Numerical Results	18
<b>5</b>	<b>Large Mass – Heat Kernel Expansion</b>	<b>19</b>
5.1	Structure of the Expansion	19
5.2	Heat Kernel Expansion Order by Order – Numerical Results	21
<b>6</b>	<b>Interpolation and Application to the Susceptibility</b>	<b>26</b>
<b>A</b>	<b>Partial Differential Equation</b>	<b>31</b>
<b>B</b>	<b>Boundary Condition – Dependence at large Mass</b>	<b>33</b>
<b>C</b>	<b>Diagonal Parts of the massless scalar Propagators</b>	<b>38</b>

---

## 1 Introduction and main Result

An important feature of non-abelian gauge theories in general and the theory of the strong interactions, Quantum Chromodynamics (QCD), in particular is the presence of topologically non-trivial gauge field configurations. Regarding QCD, this makes the true  $\theta$ -vacuum a superposition of infinitely many topologically-different gluon vacuum states which differ only by their topological properties. These otherwise distinct vacua are connected by the presence of topological configurations. Semi-classically, these are the *instantons* at zero temperature and the *calorons* for finite  $T > 0$ . These local, topological gauge field configurations change the global, topological properties of gluonic vacua [1, 2].

The caloron's topological charge density

$$q(x) = \frac{1}{32\pi^2} \epsilon^{\mu\nu\alpha\beta} \text{tr} \left( G^{\mu\nu}(x) G^{\alpha\beta}(x) \right) = \frac{1}{16\pi^2} \text{tr} \left( G^{\mu\nu}(x) \tilde{G}^{\mu\nu}(x) \right), \quad (1.1)$$

is given by the its (dual) field strength  $G$  ( $\tilde{G}$ ). Integrating this density over Euclidean spacetime with periodic time boundaries of extent  $\beta = T^{-1}$  (a compact spacetime without

boundary), as arises in the standard Euclidean thermal path integral [3, 4], yields an integer called the caloron number or topological charge  $\mathbb{Z} \in n = \int_0^\beta d\tau \int_{\mathbb{R}^3} d^3x q(\vec{x}, \tau)$  [5].

The physical  $\theta$ -vacuum and the presence of calorons require one to add the topological term  $\mathcal{L}_{\text{top}} = -i\theta q(x)$ ,  $\theta \in [-\pi, \pi]$  to the QCD Lagrangian. Because  $q \propto \vec{E} \cdot \vec{B}$ , the pure phase  $\mathcal{L}_{\text{top}}$  gives rise to a violation of the  $\mathcal{CP}$ - or  $\mathcal{T}$ -symmetry in the path integral. From studying the neutron electric dipole moment, for example,  $\mathcal{CP}$ -violating strong interaction effects are known experimentally to be extremely small, setting an upper bound  $-1.52(71) \cdot 10^{-18} \theta e \cdot \text{m} \leq 1.8 \cdot 10^{-28} e \cdot \text{m}$ , i.e.,  $|\theta| \leq 1.2 \cdot 10^{-10}$  [6, 7]. This especially tight bound on  $\theta$  is known as the strong  $\mathcal{CP}$  problem: since neither  $\mathcal{CP}$  nor  $\mathcal{T}$  are fundamental symmetries of nature, there is no fundamental reason for this fine-tuning of  $\theta$ .

A very promising solution of the strong  $\mathcal{CP}$  problem is the extension of the standard model in terms of the axion [8, 9]. For this, a high temperature  $U(1)_{\text{Peccei Quinn}}$ -symmetry [10, 11] is introduced, which is spontaneously broken at some very high energy scale  $10^8 \text{ GeV} \lesssim f_a \lesssim 10^{17} \text{ GeV}$  [12–14]. The axion  $a$  is the associated Nambu-Goldstone boson. At low temperatures  $T \lesssim \Lambda_{\text{QCD}}$ , the axion obtains a very weak coupling  $\propto f_a^{-1}$  (“invisible axion”) to gluons via topological terms and settles into its vacuum expectation value  $\langle a \rangle = -\theta f_a$ , thus also picking up a very small mass  $m_a \propto f_a^{-1}$ . Thereby, the axion modifies  $\theta$  as  $\theta \rightarrow \theta_{\text{eff}} = \theta + \frac{\langle a \rangle}{f_a} = 0$ . This means that  $\mathcal{CP}$ -conservation of QCD is dynamically ensured at the cost of introducing the axion into the theory.

The strong  $f_a^{-1}$ -suppression of all axion interactions makes it a promising dark matter candidate<sup>1</sup> [16–19]. Determining its mass and cosmological abundance requires understanding the temperature dependence of the topological susceptibility

$$\chi_{\text{top}}(T) = \int d^4x \langle q(x)q(0) \rangle_T = -\frac{1}{\beta V} \left. \frac{\partial^2 \ln(Z(\theta))}{\partial \theta^2} \right|_{\theta=0}, \quad (1.2)$$

where  $Z$  is the partition function and  $\beta V$  is the volume of spacetime. Indeed, the axion mass depends on  $\chi_{\text{top}}$  via

$$m_a(T) = \frac{\sqrt{\chi_{\text{top}}(T)}}{f_a}. \quad (1.3)$$

For  $T = 0$ , chiral perturbation theory gives a reliable tool for computing  $\chi_{\text{top}}$  and precise results are available:  $\sqrt[4]{\chi_{\text{top}}(0)} = (75.5 \pm 0.5) \text{ MeV}$  [13, 20–22]. As a result, the axion mass is  $m_a(0) = (5.69 \pm 0.05) \mu\text{eV} \left( \frac{10^{12} \text{ GeV}}{f_a} \right)$  [20].

Evaluating the topological susceptibility well above the QCD crossover temperature  $T_c \simeq 155 \text{ MeV}$  [23, 24] is more challenging, but axion cosmology requires precise results: [25] shows that the cosmological history of the axion depends critically on  $\chi_{\text{top}}(T)$  in the temperature range  $400 \text{ MeV} \lesssim T \lesssim 1.1 \text{ GeV}$ . In this temperature range,  $\chi_{\text{top}}$  is small and dominated by isolated topological objects. Semiclassically, these would be the *Harrington-Shepard* (HS) (*anti-*) calorons [26] with  $n = \pm 1$ . Unfortunately, the HS caloron density cannot reliably be determined perturbatively, requiring a lattice investigation instead. Both existing lattice investigations in this temperature range [22] and any future investigations

<sup>1</sup>As of yet, the axion is still a hypothetical particle lacking verification by observation, but many experiments focusing on axion dark matter are ongoing or planned [15].

using topology reweighting techniques [27, 28] will be performed in so-called  $2 + 1 + 1$  simulations, meaning that the up, down, strange, and charm quarks are included, but the bottom quark is not. Indeed, we are not aware of any lattice simulations at physical quark masses which include dynamical bottom quarks - and adding them to the existing simulation framework would require very significant additional work. At the highest temperatures mentioned above, however, it is not clear that the bottom quark can be considered heavy compared to the thermal scale; it may influence the topological susceptibility.

Therefore, we address the question of how adding a dynamical  $b$  quark alters the topological susceptibility of finite-temperature  $2 + 1 + 1 + 1$  theory compared to the  $2 + 1 + 1$  case accessible to lattice QCD. The two theories should be compared keeping the infrared physics fixed, e.g., at the same value of the strong coupling in the  $2 + 1 + 1$ -flavor effective infrared theory. We do this by computing the ratio of the topological susceptibility in the dilute caloron gas model with a  $b$  quark at the physical mass, and the susceptibility in the same model but with the  $b$  quark taken to be asymptotically heavy. We match the coupling so that the two theories coincide in the IR. The assumption is then that the effect of a heavy quark on a caloron suitably captures its effect on the somewhat messier topological objects which matter at physical coupling values.

Figure 1 shows our main result concerning this question. We show the temperature-dependent ratio  $\kappa = \frac{\chi_{\text{top}}(m_b)}{\chi_{\text{top}}(m_{b, \text{asy}})}$  of the topological susceptibilities for theories with physical and asymptotic  $b$ -masses, respectively. As throughout this work,  $m \hat{=} \frac{m}{T}$  stands for the dimensionful mass rescaled by the temperature. We see that for the physically interesting temperature range  $400 \text{ MeV} \lesssim T \lesssim 1.1 \text{ GeV}$  (i.e., the temperature most important for the cosmological history of axions, see [25]) and thus the mass range  $4 \lesssim m_b \lesssim 10$ , the difference between the physically heavy  $b$  and its asymptotically heavy counterpart used in lattice QCD is  $\lesssim 5\%$ . Only for high temperatures  $m_b \lesssim 2$  do we see an appreciable ( $\gtrsim 10\%$ ) difference between the topological susceptibilities of finite-temperature  $2 + 1 + 1 + 1$  theory (including a dynamical  $b$  quark) and the  $2 + 1 + 1$  case of lattice QCD.

The remaining article shows our derivation of this and other results. It is organized as follows: in the preliminaries we give a short overview over calorons and how they enter into QCD, how the partition function and consequently the topological susceptibility are related to the caloron density and how we incorporate heavy quarks at finite temperature. In section 3 we outline in more detail our strategy for dealing with different quark mass regimes and the interpolation between them. In section 4 we then calculate the caloron density for light, but non-vanishing quark masses and in section 5 for heavy quarks. In section 6 we perform the interpolation between these mass regimes to obtain the caloron density for general quark masses and finally calculate the topological susceptibility ratio.

**Conventions:** We employ a system of natural units with  $c = \hbar = k_B = 1$ . We work in Euclidean, finite- $T$  spacetime  $\mathbb{R}^3 \times S^1_{\text{rad}=1/2\pi}$  with coordinates  $x^\mu = (\vec{x}, \tau)$ ,  $\mu = 1, \dots, 4$  and  $i = 1, 2, 3$ . All length scales, masses, energies, etc. are rescaled by appropriate factors of  $\beta = T^{-1}$  to be dimensionless. By  $[q]$  we denote the mass-dimension of the corresponding dimensionful quantities  $q$ . Furthermore, when there is a caloron present, we choose

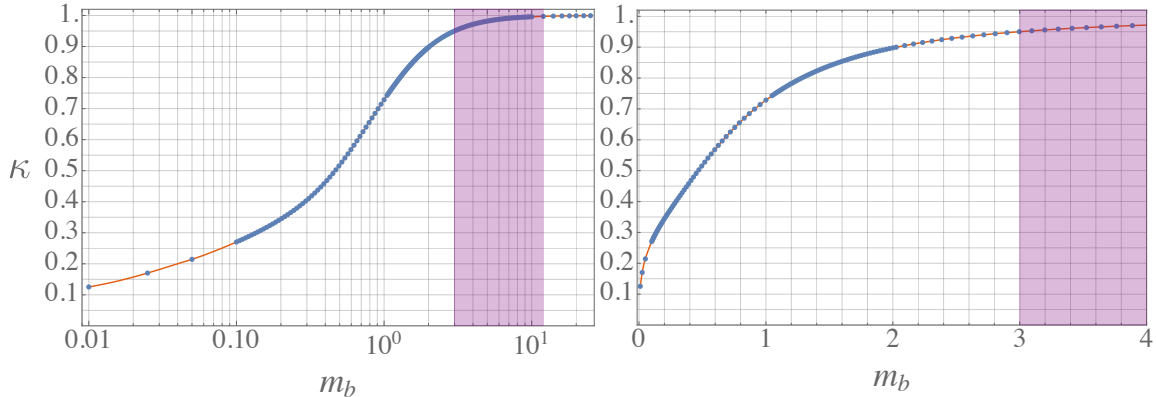


**Figure 1:** The ratio of topological susceptibilities  $\kappa(m_b, 4, 1, 3)$  (6.14) comparing a theory with a four light and a physical  $b$  quark in  $SU(3)$  gauge theory to lattice QCD, where the  $b$  quark is asymptotically heavy. Due to the modification of the running coupling (3.9),  $\kappa$  depends only on the physical quark mass  $m_b$ . The interesting mass range  $3 \lesssim m_b \lesssim 12$ , chosen to be slightly wider than the physically relevant temperature range  $400 \text{ MeV} \lesssim T \lesssim 1.1 \text{ GeV}$  - given a dimensionful  $b$ -mass  $m_b \approx 4.2 \text{ MeV}$  [29] -, is marked in purple.

coordinates for  $\mathbb{R}^3 \times S_{\text{rad}=1/2\pi}^1$  so that the caloron is at the center, e.g., the caloron center is located at  $(\vec{x}, \tau) = (\vec{0}, 0)$ . All properties tied to the appropriately dimensionless, Euclidean  $T = 0$ -spacetime  $\mathbb{R}^4$  are denoted as barred, e.g.:  $\bar{x}^\mu = (\vec{\bar{x}}, \bar{t})$ . The  $T > 0$  and  $T = 0$  radii are defined as  $r = \sqrt{x^i x^i}$  and  $\bar{r} = \sqrt{\bar{x}^\mu \bar{x}^\mu}$ , respectively. The unit vector in the  $\mu$ -direction is written as  $\hat{e}_\mu$ . We abbreviate the spacetime integral  $\int^1 d^4x = \int_0^1 d\tau \int_{\mathbb{R}^3} dx^3$  and the operator trace  $\text{Tr}(\cdot) = \int^1 d^4x \text{tr}_{\text{Dirac, color, etc.}}(\cdot)$ . We consider  $SU(N)$  gauge theory and  $N_f$  quark flavors and specify  $N$  and  $N_f$  only when computing concrete results. We employ the geometrical normalization of the gauge covariant derivative  $D = \partial - iA$  and occasionally use the short-hand notation:  $D^\mu q^{\nu_1 \dots \nu_n} = q^{\nu_1 \dots \nu_n; \mu}$ . The four Pauli matrices are denoted as  $\sigma^\mu = (\vec{\sigma}, i)$  with roman indices  $\sigma^a$  running from 1 to 3. We abbreviate  $\vec{x} \cdot \vec{\sigma} = r \hat{e}_r(x) \cdot \vec{\sigma} = r \sigma^r(\theta, \varphi)$ . We choose anti-Hermitian Euclidean  $\gamma$ -matrices  $\gamma^{\mu\dagger} = -\gamma^\mu$  which satisfy the Clifford algebra  $\{\gamma^\mu, \gamma^\nu\} = -2\delta^{\mu\nu}$ . To avoid confusion with the gamma function, we denote the quantum effective action by  $\tilde{\Gamma}$ .  $\gamma_E = 0.57721\dots$  is the Euler-Mascheroni constant. Lastly, we include 0 in the natural numbers  $\mathbb{N} = \{0, 1, 2, \dots\}$  (mainly used for summation).

## 2 Preliminaries

As stated in section 1, we are interested in obtaining the topological susceptibility (1.2)  $\chi_{\text{top}}(m_f, T) = -\frac{1}{V} \left. \frac{\partial^2 \ln(Z(\theta))}{\partial \theta^2} \right|_{\theta=0}$ , with  $V = \text{vol}(\mathbb{R}^3 \times S_{\text{rad}=1/2\pi}^1)$  the volume of spacetime (the spacetime  $\mathbb{R}^3 \times S_{\text{rad}=1/2\pi}^1$  is periodic in the temperature direction with fermions experiencing anti-periodic boundary conditions.), for  $2 + 1 + 1 + 1$  theory at finite temperature including a dynamical  $b$  quark.

As we discuss later, it suffices to consider only the aforementioned HS calorons [26]:

$$A_{\text{HS}} = -\bar{\eta}^{a\mu\nu} \partial^\nu \ln(\phi(x)) \frac{\sigma^a}{2} \quad \text{with} \quad (2.1)$$

$$\phi(x) = 1 + \frac{\pi \varrho^2 \sinh(2\pi r)}{r(\cosh(2\pi r) - \cos(2\pi\tau))} \quad (2.2)$$

given in singular gauge (i.e., all topological information is “stored” at the caloron center). Here  $\bar{\eta}$  is the anti-’t Hooft symbol [30, 31] and  $\varrho$  gives the ( $\beta$ -rescaled) size of the caloron placed at  $(\vec{0}, 0)$ . For the HS anti-caloron the anti-’t Hooft symbol  $\bar{\eta}$  in (2.1) is replaced by the ’t Hooft symbol  $\eta$ .

Calorons can be written as sums of infinitely many, uniformly spaced instantons placed at  $\mathbb{R}^4 \ni 0 + j\hat{e}_4$ ,  $j \in \mathbb{Z}$ . In particular, HS calorons can be written as a sum over infinitely many *Belavin-Polyakov-Schwartz-Tyupkin* (BPST) *instantons*.<sup>2</sup> Instantons approach pure gauge form at infinity  $\lim_{\bar{r} \rightarrow \infty} A_{\text{inst}} = i\Omega\partial\Omega^{-1} \in \mathfrak{su}(N)$  with  $\Omega \in SU(N)$ , which serves to restrict the gauge configurations  $\lim_{\bar{r} \rightarrow \infty} \Omega = 1$  and compactify  $\mathbb{R}^4$  to an infinite 3-sphere  $S^3$ . According to a theorem by Bott [32], the “topologically active” part of such maps  $\Omega : S^3 \rightarrow SU(N)$  (or any simple Lie group) is only a subgroup  $SU(2) \subset SU(N)$ . Therefore, HS calorons are fully determined by the  $\mathfrak{su}(2)$ -object (2.1), embedded in an  $\mathfrak{su}(N)$ -matrix

$$A_{\text{HS}, \mathfrak{su}(N)} = \left( \begin{array}{c|c} A_{\text{HS}} & 0_{2 \times (N-2)} \\ \hline 0_{(N-2) \times 2} & 0_{(N-2) \times (N-2)} \end{array} \right), \quad (2.3)$$

together with two residual symmetry groups: one group of global (“rigid”)  $SU(2)$ -transformations acting on  $A_{\text{HS}}$  that leave the caloron invariant and one group of  $\frac{SU(N)}{SU(N-2) \times U(1)}$ -transformations of  $A_{\text{HS}, \mathfrak{su}(N)}$  that only change the embedding [33, 34].

In the limit of small distances  $|(\vec{x}, \tau)| \ll 1$  the HS caloron (2.1) takes the form of a BPST instanton

$$A_{\text{HS}}^\mu \stackrel{|x| \ll 1}{\cong} \bar{\eta}^{a\mu\nu} \frac{2\tilde{\varrho}^2}{x^2} \frac{x^\nu}{x^2 + \tilde{\varrho}^2} \frac{\sigma^a}{2} \left( 1 + \mathcal{O}(|x|^4) \right) \quad (2.4)$$

with modified, reduced size

$$\tilde{\varrho} = \frac{\varrho}{\sqrt{1 + \frac{\pi^2 \varrho^2}{3}}}. \quad (2.5)$$

This means that on length scales much smaller than the temperature/periodicity scale the caloron is identical to an instanton with modified size  $\tilde{\varrho}$  and the actual periodicity of  $\mathbb{R}^3 \times S^1_{\text{rad}=1/2\pi}$  is concealed in the far distance [5].

(Anti-)Calorons are (anti-)self-dual ( $\tilde{G}^{\mu\nu} G^{\mu\nu} = \pm G^{\mu\nu}$ ) solutions to the classical equations of motion  $D^\mu G^{\mu\nu} = 0$  and can be treated as a classical, stationary background for quantization, i.e, the gauge, quark and Faddeev-Popov ghost fields of the QCD-system are of the form  $A^\mu = A_{\text{HS}, \mathfrak{su}(N)}^\mu + A_{\text{quantum}}^\mu$ ,  $\psi = \psi_{\text{quantum}}$  and  $c = c_{\text{quantum}}$ , respectively. One then also enforces the background gauge condition  $D^\mu(A_{\text{HS}, \mathfrak{su}(N)})A_{\text{qm}}^\mu = 0$  to eliminate residual gauge freedom in the fluctuations [30, 31].

---

<sup>2</sup>BPST instantons [1] are of the same form as (2.1), but with  $\phi_{\text{BPST}}(\vec{x}, \vec{z}) = 1 + \frac{\varrho^2}{(\vec{x} - \vec{z})^2}$ , where  $\vec{z}$  is the instanton center. The HS caloron is then constructed by  $\phi(x) = \sum_{j \in \mathbb{Z}} \phi_{\text{BPST}}(\vec{x}, 0 + j\hat{e}_4)$ .

Using Laplace’s method for the integration with respect to the quantum fluctuations, the regularized, vacuum-normalized partition function and effective action  $\tilde{\Gamma}$  up to first loop order in the quantum fluctuations  $A_{\text{qm}}, \psi_{\text{qm}}, c_{\text{qm}}$  in a classical HS caloron background - i.e., up to  $\mathcal{O}((\text{qm. fluct.})^2)$  -, including the topological term (1.1), are [5, 30, 31, 35]

$$Z(\theta) = e^{i\theta} V \mathcal{D} = \exp(-\tilde{\Gamma}(\theta)), \quad \mathcal{D} = \int_0^\infty d\varrho \mathcal{d}(\varrho) = \int_0^\infty d\varrho e^{-\gamma(\varrho)}, \quad (2.6)$$

$$\begin{aligned} \mathcal{d}(m_f, \varrho, \lambda) &= \frac{2^{2-2N} e^{-\frac{8\pi^2}{g^2}}}{\pi^2(N-1)!(N-2)!} \left(\frac{8\pi^2}{g^2}\right)^{2N} \varrho^{4N-5} \lambda^{4N} \sqrt{\frac{\det' \mathfrak{M}_A(\lambda) \det' \mathfrak{M}_{A,0}}{\det' \mathfrak{M}_A \det' \mathfrak{M}_{A,0}(\lambda)}} \times \\ &\times \frac{\det \mathfrak{M}_{\text{gh}} \det \mathfrak{M}_{\text{gh},0}(\lambda)}{\det \mathfrak{M}_{\text{gh}}(\lambda) \det \mathfrak{M}_{\text{gh},0}} \prod_f \frac{m_f}{\lambda} \left( \frac{\det(-D_-^2 + m_f^2) \det(-\partial_-^2 + \lambda^2)}{\det(-D_-^2 + \lambda^2) \det(-\partial_-^2 + m_f^2)} \right)^2, \end{aligned} \quad (2.7)$$

where  $\mathcal{D}$  and  $\mathcal{d}(\varrho)$  are the caloron density and caloron density/likelihood per size, respectively, and  $\gamma(\varrho)$  is the negative logarithmic caloron density<sup>3</sup>. The caloron density  $\mathcal{D}$  can be understood as the mean-squared topology per unit volume, and  $\mathcal{d}$  its integrand when  $\mathcal{D}$  is expressed as an integral over caloron size  $\varrho$ . The gluon and ghost field differential operators are  $\mathfrak{M}_A^{\mu\nu} = \left(-D_+^2(A_{\text{HS}, \text{su}(N)}^\mu) \delta^{\mu\nu} - 2G_{\text{su}(N)}^{\mu\nu}\right)_{\text{adj}}$  and  $\mathfrak{M}_{\text{gh}} = -D_{+, \text{adj}}^2(A_{\text{HS}, \text{su}(N)}^\mu)$ , respectively, where “adj” stands for the adjoint representation. The subscript “0” denotes the free, vacuum case without a caloron background and the subscripts “+/-” denote  $\tau$ -periodicity/anti-periodicity of the respective eigenfunctions. The fermionic differential operator  $i\not{D}(A_{\text{HS}, \text{su}(N)}^\mu) + m_f$  was translated to a Klein-Gordon operator  $-D_-^2 + m_f^2$  of an anti-periodic scalar in the determinant, which is unique to (anti-)self dual gauge fields [36, 37].  $\lambda$  is the renormalization energy scale.

Since the BPST and thus the HS solution to the self-duality condition as well as the general Atiyah-Drinfeld-Hitchin-Manin (ADHM) construction of such solutions [38] are all limited to 4-dimensional spacetime, dimensional regularization methods are not available in a theory with a classical caloron background, as there is no known expression for calorons in  $4-2\epsilon$ -dimensional spacetime. Instead, regularization is achieved by employing the Pauli-Villars method which introduces additional copies of all quantum fields with large mass  $\lambda$  and minimal coupling only to the background. This means adding mass terms  $\mathfrak{M}_{A, \text{gh}}(\lambda) = \mathfrak{M}_{A, \text{gh}} + \lambda^2$ . An alternative interpretation is that we are comparing the topology density to the topology density at an extremely large quark mass  $\lambda$ . Ultraviolet divergences cancel in the difference between these two theories.

In [30, 31] the determinant ratios in (2.7) were obtained for the simplified case of zero temperature and vanishingly light fermions  $0 < m\varrho \ll 1$  and the connection to dimensional

---

<sup>3</sup>denoted by  $\gamma$  since  $\exp(-\tilde{\Gamma}(\theta)) = e^{i\theta} V \int_0^\infty d\varrho \exp(-\gamma)$

regularization was established. The instanton density for  $N_f$  vanishingly light quarks reads

$$d = \frac{2e^{-\alpha(1)+4\alpha(\frac{1}{2})+\ln 2-N(2\alpha(\frac{1}{2})+2\ln 2)+2N_f\alpha(\frac{1}{2})}}{\pi^2(N-1)!(N-2)!} \left(\frac{8\pi^2}{g^2}\right)^{2N} e^{-\frac{8\pi^2}{g^2(1/\varrho)}} \frac{\prod_f m_f \varrho}{\varrho^5} \quad (2.8)$$

$$\text{with the running coupling } \frac{8\pi^2}{g^2(1/\varrho)} = -\frac{1}{3} \ln(\lambda\varrho)(11N - 2N_f) \quad (2.9)$$

and  $\alpha(\frac{1}{2}) \approx 0.145873$  and  $\alpha(1) \approx 0.443307$ . Here  $m_f$ ,  $\lambda$  and  $\varrho$  can be understood as the non-rescaled, dimensionful quantities at  $T = 0$ . Usually, the factor  $g^{-4N}$  in (2.8) is “manually” replaced by the running coupling at scale  $\varrho^{-1}$  (2.9), which is identified in the exponent during the calculation of (2.8). However, as we argue below (2.11) for  $T = 0$  and as show in figure 12 for  $T > 0$ , this is a higher order effect and we thus choose to neglect this correction when calculating the topological susceptibility, since  $\chi_{\text{top}}$  in its known form is itself based on calculations only up to  $\mathcal{O}((\text{qm. fluct.})^2)$ , i.e., 1-loop order (cf. (2.7)).

In order to extend (2.8) to the physically interesting case of  $T > 0$  and  $m_f \varrho \ll 1$  as well as  $m_f \ll 1$ , the determinant relations must be reevaluated for these new parameters. For that the determinant relations in (2.7) are split into the parts with  $T = 0$ ,  $m_f \varrho \ll 1$  and a correction factor  $f$ :

$$d(m_f, \varrho, \lambda) = d(m_f \varrho \ll 1, \varrho, \lambda)|_{T=0} f(m_f, \varrho)|_{T>0}. \quad (2.10)$$

This was established in [5], where it was also shown that (2.8) still holds at  $T > 0$ .

For finite temperatures this correction factor due to gluons and  $N_f$  vanishingly light fermions was calculated in [5] and reads  $f(m_f \ll 1 \wedge m_f \varrho \ll 1, \varrho) = f(m_f = 0, \varrho)$ :

$$f(0, \varrho)|_{T>0} = \exp\left(-\frac{(\pi\varrho)^2}{3}(2N + N_f) - A(\pi\varrho)(12 + 2(N - N_f))\right) \quad (2.11)$$

with  $A(x) \approx -\frac{1}{12} \ln\left(1 + \frac{x^2}{3}\right) + a_1\left(1 + \frac{a_2}{x^{3/2}}\right)^{-8}$ ,  $a_1 \approx 0.01289764$  and  $a_2 \approx 0.15858$ . From (2.11) one can deduce that large calorons  $\varrho \gtrsim 0.8$  are exponentially unfavorable, while (2.8) shows that small calorons  $\varrho \lesssim 0.1$  are polynomially suppressed. The preferred caloron density size is  $\varrho \approx 0.42$  in pure glue with  $N = 3$  and goes down to  $\varrho \approx 0.34$  for  $N_f = 4$ . From this preferred caloron size we can deduce that the replacement  $g^{-4N} \rightarrow g^{-4N}(1/\varrho)$  in (2.8) adds only small corrections: the large Pauli-Villars mass  $\lambda \gg 1$  (the regularization energy scale in  $\overline{\text{MS}}$ ) yields  $(\ln(\lambda\varrho))^{2N} = (\ln \lambda)^{2N}(1 + 2N\epsilon + \mathcal{O}(\epsilon^2))$ ,  $\epsilon = \frac{\ln \varrho}{\ln \lambda}$ . Therefore, we choose to neglect the  $\varrho$ -dependent  $\epsilon$ -corrections and keep only the “constant”, i.e.,  $\varrho$ -independent, term  $\ln \lambda$  when calculating  $\chi_{\text{top}}$ . We verify this simplification for our system with a heavy  $b$  quark in figure 12.

These small caloron sizes allows us to use the *small-constituent approximation* at high enough temperatures, i.e., to describe an  $n$ -caloron configurations as superpositions of spatially well-separated and thus non-interacting<sup>4</sup> single HS (anti-)calorons. At leading order, all higher charge-calorons can then be described this way. A general caloron

<sup>4</sup>Instanton and caloron interactions are short-ranged; e.g., for well-separated instantons at locations  $z_i$  with typical separation scale  $d$ , the interaction corrections compared to an exact solution are  $\lesssim \frac{\varrho^2}{d^3}$  in the “near region”  $|x - z_i| \lesssim \varrho$  (for some  $i$ ) and  $\lesssim \frac{\varrho^4}{d^5}$  in the “far region”  $|x - z_i| \gtrsim \varrho \forall i$  [39].



background is then populated by calorons of all  $n \in \mathbb{Z}$  and one describes  $n$ -caloron configurations using  $n_+$  HS calorons and  $n_-$  HS anti-calorons with  $n_+ - n_- = n$ . This is the *dilute gas approximation* (DGA) [35, 40]. In this approximation, the partition function and thus the topological susceptibility take a simple form:

$$Z_{\text{DGA}}(\theta) = \exp(2\beta V \mathcal{D}(T, m_f) \cos(\theta)), \quad (2.12)$$

$$\Rightarrow \chi_{\text{top}}(T > T_c) \stackrel{\text{DGA}}{=} 2\mathcal{D}(T, m_f) = 2 \int_0^\infty d\varrho \mathcal{d}(m_f, \varrho, \lambda), \quad (2.13)$$

where  $T_c \simeq 155$  MeV is the critical temperature of chiral perturbation theory [23, 24].

For zero temperature but non-vanishing fermion masses, the fermion determinant relation was evaluated and one has analytical results for small-mass and large-mass expansions

$$f_{\text{ferm}}(m_f, \varrho)|_{T=0} = \begin{cases} \prod_f \exp\left(m_f^2 \varrho^2 \ln(m_f \varrho) + (\gamma_E - \ln 2)m_f^2 \varrho^2\right) & : m_f \varrho \lesssim 0.5 \\ \prod_f \frac{e^{-2\alpha(\frac{1}{2})}}{(m_f \varrho)^{\frac{1}{3}}} \exp\left(-\frac{2}{75(m_f \varrho)^2} - \frac{34}{735(m_f \varrho)^4} + \right. \\ \quad \left. + \frac{464}{2835(m_f \varrho)^6} - \frac{15832}{148225(m_f \varrho)^8}\right) & : m_f \varrho \gtrsim 1.8 \end{cases} \quad (2.14)$$

as well as an interpolation between them, covering arbitrary masses, in [41]:

$$\begin{aligned} f_{\text{ferm}}(m_f, \varrho)|_{T=0} &= \\ &= \prod_f \frac{e^{-2\alpha(\frac{1}{2})}}{(m_f \varrho)^{\frac{1}{3}}} \exp\left(\frac{\frac{1}{3} \ln(m_f \varrho) + 2\alpha(\frac{1}{2}) - (6\alpha(\frac{1}{2}) - \gamma_E + \ln 2)(m_f \varrho^2) - \frac{2}{5}(m_f \varrho)^4}{1 - 3(m_f \varrho)^2 + 20(m_f \varrho)^4 + 15(m_f \varrho)^6}\right). \end{aligned} \quad (2.15)$$

Furthermore, an explicit numerical solution covering arbitrary masses was found [42]:

$$\begin{aligned} f_{\text{ferm}}(m_f, \varrho)|_{T=0} &= \\ &= \prod_f \exp\left(-2\alpha\left(\frac{1}{2}\right) - 2 \lim_{L \rightarrow \infty} \left( \sum_{l=0, \frac{1}{2}, \dots}^L (2l+1)(2l+2) P_{M_f, \varrho}(l) + 2L^2 + 4L - \right. \right. \\ &\quad \left. \left. - \left(\frac{1}{6} + \frac{m_f^2 \varrho^2}{2}\right) \ln(L) + \frac{m_f^2 \varrho^2}{2} (\ln(m_f \varrho) + 1 - 2 \ln 2) + \frac{127}{72} - \frac{\ln 2}{3} \right)\right), \end{aligned} \quad (2.16)$$

where  $P_{M_f, \varrho}(l) = S_{M_f, \varrho}^{l, l+\frac{1}{2}}(\bar{r} \rightarrow \infty) + S_{M_f, \varrho}^{l+\frac{1}{2}, l}(\bar{r} \rightarrow \infty)$  and  $S_{M_f, \varrho}^{l, j}(\bar{r})$  is the numerical solution to the ordinary differential equation

$$d_{\bar{r}}^2 S^{l, j} + (d_{\bar{r}} S^{l, j})^2 + \left(\frac{1}{\bar{r}} + 2 \frac{d_{\bar{r}} I_{2l+1}(m_f \bar{r})}{I_{2l+1}(m_f \bar{r})}\right) d_{\bar{r}} S^{l, j} = \frac{4(j-l)(j+l+1)}{\bar{r}^2 + \varrho^2} - \frac{3\varrho^2}{(\bar{r}^2 + \varrho^2)^2}, \quad (2.17)$$

with  $I_\alpha(x)$  the modified Bessel function of the first kind.

We aim to calculate the correction factor  $f(m_f, \varrho)|_{T>0}$  for the general case of massive quarks at finite temperature. For that, we calculate the regularized, vacuum-normalized Klein-Gordon operator determinant with anti-periodic temporal boundaries from (2.7):

$$-\ln(f_{\text{ferm}}) = \gamma_{\text{ferm}} \supset -2 \ln \left( \frac{\det(-D_-^2 + m^2) \det(-\partial_-^2 + \lambda^2)}{\det(-D_-^2 + \lambda^2) \det(-\partial_-^2 + m^2)} \right) = -2\gamma_{s, -}. \quad (2.18)$$

As in (2.14) - (2.16), which only consider the  $\mathfrak{su}(2)$ -caloron, we can also limit ourselves to  $D(A_{\text{HS}})$  in (2.18). This is justified by (2.3) and the connection to  $m = 0$ , which contains the right  $SU(N)$ -dependent factors, cf. (2.8) and (2.11).

The finite- $T$  spacetime  $\mathbb{R}^3 \times S_{\text{rad}=1/2\pi}^1$  has a distinct, bounded time direction compared to the unbounded space directions. This breaks the  $SO(4)$ -symmetry of  $T = 0$ -physics down to  $SO(3)$ . From the physical point of view, the presence of the external heat bath implies a preferred Lorentz frame, the heat bath's rest frame. Therefore, Lorentz invariance is broken: rotations and translations are still symmetries, whereas boosts are not, and the Lorentz group  $SO^+(1, 3)$  is broken to  $SO(3)$  [43, 44]. As the HS caloron, compared to the BPST instanton, is only radially symmetric in the three space dimensions (and not explicitly so, cf. (2.1), (2.2)), calculating  $\det(-D_-^2 + m_f^2)$  requires solving a complicated 2-dimensional (partial) differential equation - we obtain this equation appendix A -, compared the 1-dimensional ordinary differential equation at  $T = 0$  (2.17). We instead follow an alternative which was first used for  $T = 0$  in [41] and that we adapt and generalize to finite temperatures. Our approach is discussed in detail in the following section 3.

### 3 Strategy of our Approach

As we stated in section 1, we want to compare topological susceptibilities for theories with  $2 + 1 + 1 + 1$  (including a dynamical  $b$  quark) and  $2 + 1 + 1$  dynamical quarks (with  $b$  asymptotically heavy, accessible via lattice QCD). For that, we calculate  $\chi_{\text{top}}(m_f, T)$  using (2.13), once with physical  $m_b$  and once with an asymptotic  $m_{\text{asy}}$ , keeping the 4-flavor effective theories in the IR fixed, i.e., equal for both cases. Then we compute the ratio  $\frac{\chi_{\text{top}}(m_b, T)}{\chi_{\text{top}}(m_{\text{asy}}, T)}$  which, together with the 4-flavor lattice result, gives the full 5-flavor topological susceptibility at high temperatures.

In order to obtain the caloron density, as required in (2.13), we to obtain the fermionic part of the caloron density correction factor (cf. (2.10)) in the general case of heavy quarks at finite temperatures. For this, we proceed as follows:

#### Step 1)

We calculate  $\gamma_{s, -}$  (2.18) for small (but non-vanishing) and large fermion masses separately and obtain two expansions, analogous to (2.14):

$$f_{\text{ferm}}(m_f, \varrho)|_{T>0} = \begin{cases} f_{\text{small}} = \exp(2\gamma_{s, -}(m, \varrho)) & : \text{small } m \\ f_{\text{large}} = \frac{e^{-2\alpha(\frac{1}{2})}}{(\lambda\rho)^{\frac{1}{3}}} \exp(2\gamma_{s, -}(m, \varrho, \lambda)) & : \text{large } m \end{cases}. \quad (3.1)$$

The large- $m$  factor  $e^{-2\alpha(1/2)}(\lambda\rho)^{-1/3}$  cancels  $m \ll 1$ -terms in (2.8).

For small fermion masses  $m \ll 1$  we Taylor expand (2.18) up to first order in  $m^2$ . Such a Taylor expansion is not possible at zero temperature, where the known result for  $\gamma_{s,-}$  contains a term  $(m\varrho)^2 \ln(m\varrho)$  [41] which is non-analytical at  $m\varrho = 0$ . Noting that  $\ln \det(-\bar{D}^2 + m^2) = \text{Tr} \ln(-\bar{D}^2 + m^2)$ , this IR non-analyticity can be traced back to eigenmodes of  $-\bar{D}^2$  with arbitrarily low momenta that get affected arbitrarily strongly by the introduction of even an infinitesimal mass. At finite temperature, however, fermions have anti-periodic boundary conditions which raise the lowest fluctuation frequencies in  $D_-^2$  to  $\pi T$ , the lowest fermionic Matsubara frequency, or  $\pi$  in our dimensionless units. Therefore, as long as  $m \ll 1$ , the introduction of a small mass has only an infinitesimal effect on the determinant. Indeed, one expects the small-mass expansion to be a Taylor series with a radius of convergence  $\sim \pi$ . In section 4 we thus obtain a Taylor expansion of the general structure

$$\gamma_{\text{ferm}}(m \text{ small}, \varrho) = -2\gamma_{s,-}(m \text{ small}, \varrho) = \frac{(\pi\varrho)^2}{3} - 2A(\pi\varrho) - 2m^2 \gamma_{s,-}^{\text{small}}(\varrho) + \mathcal{O}(m^4), \quad (3.2)$$

where the purely  $\varrho$ -dependent first terms are given by the fermionic part of the known result (2.11). Computing the  $m^4$ -coefficient is possible in principle but much more challenging than the  $m^2$ -coefficient and we will not attempt it here.

For large quark masses  $m \gg 1$  we employ the asymptotic *heat kernel expansion* of (2.18). In section 5 we find the resulting expansion

$$\gamma_{s,-}(m \text{ large}, \varrho, \lambda) = \frac{1}{6} \ln\left(\frac{\lambda}{m}\right) + \sum_{k=1}^{k_{\text{max}}} \frac{\gamma_{s,-}^{\text{large}, k}(\varrho)}{m^{2k}}. \quad (3.3)$$

The series is asymptotic and its Borel resummation contains an ambiguity  $\sim m^b e^{-m}$ ,  $b \sim 1$ , which is sensitive to the anti-periodic boundary conditions (we discuss this in appendix B).

### Step 2)

We interpolate between the small-mass result (3.2) and the large-mass result (3.3) in order to obtain the full correction factor following (3.1). For this we seek an approximate fitting function for  $\gamma_{\text{ferm}}$  which matches both limiting behaviors. Specifically, we seek a function  $p(m, \varrho)$  defined as

$$-\ln(f_{\text{ferm}}(m, \varrho)) = \gamma_{\text{ferm}} = 2\alpha\left(\frac{1}{2}\right) + p(m, \varrho) \quad (3.4)$$

obeying

$$p(m, \varrho) \rightarrow \begin{cases} -2\alpha\left(\frac{1}{2}\right) + \frac{(\pi\varrho)^2}{3} - 2A(\pi\varrho) - 2m^2 \gamma_{s,-}^{\text{small}}(\varrho) & : \text{small } m \\ \frac{1}{3} \ln(m\varrho) - 2 \sum_{k=1}^{k_{\text{max}}} \frac{\gamma_{s,-}^{\text{large}, k}(\varrho)}{m^{2k}} & : \text{large } m \end{cases}. \quad (3.5)$$

Because the large-mass behavior features a logarithm  $\ln(m\varrho)$  while the small-mass behavior does not, a regular Padé approximant cannot work for  $p$  in (3.5); instead we make

the ‘‘Padé-like’’ approximant *Ansatz*

$$p(m, \varrho) = \frac{\sum_{i=0}^K p_i(\varrho) m^{2i}}{\prod_{j=1}^{K+1} (1 + \mathcal{P}_j(\varrho) m^2)} + \frac{1}{6} \ln(m^2 \varrho^2 + \xi^2(\varrho)), \quad \mathcal{P}_j > 0 \forall j, \varrho, \quad (3.6)$$

$$K = \begin{cases} \frac{k_{\max} - 1}{2} & : k_{\max} \text{ odd} \\ \frac{k_{\max} - 2}{2} & : k_{\max} \text{ even} \end{cases}, \quad (3.7)$$

which contains a regulated logarithmic function that becomes a simple log at large mass and a (purely  $\varrho$ -dependent) ‘‘constant’’ at small mass. The coefficients of the polynomial in the numerator, the roots of the polynomial in the denominator, and the constant in the log then represent  $2K + 3$   $\varrho$ -dependent coefficient functions. For  $m \ll 1$  this *Ansatz* approaches an  $m$ -independent function of  $\varrho$  with  $\mathcal{O}(m^2)$ -corrections. For  $m \gg 1$  the logarithm correctly reproduces the corresponding term in (3.5), while the rational part falls off as  $m^{-2}$ . To fix the coefficients, we perform a Taylor expansion of (3.6) up to  $\mathcal{O}(m^2)$  for small masses as well as a Laurent expansion up to  $\mathcal{O}(m^{-2k_{\max}})$  for large masses and identify these expansions with the corresponding ones in (3.5) by equating the  $\varrho$ -dependent coefficients. This yields a non-linear system of equations. Note that, if the number of known Taylor and Laurent expansion coefficients is even, then the *Ansatz* has the wrong number of free parameters; but in this case one can fix the value of  $\xi$ , for instance  $\xi = 1$ , and fit only the numerator and denominator coefficients.

Our approach is motivated by the excellent agreement of  $-\frac{1}{2} \ln(f_{\text{ferm}}(m_f, \varrho)|_{T=0})$  given by the interpolation (2.15) in [41] with the full numerical result (2.16) from [42] as shown in figure 6 of [42].

Having determined  $p(m, \varrho)$ , we can describe the full caloron density (2.10) using the  $T = 0$ -caloron density (2.8) and the correction factors (2.11) for  $N_{f_l}$  (vanishingly) light quarks as well as our result ((3.5), (3.6)) for  $f_{\text{ferm}}(m_{f_h}, \varrho)|_{T>0} = \exp(-2\alpha(\frac{1}{2}) - p(m_{f_h}, \varrho))$  describing  $N_{f_h}$  heavy quarks,  $N_f = N_{f_l} + N_{f_h}$ :

$$\begin{aligned} d(m_{f_l}, m_{f_h}, \varrho, \lambda) &= \frac{2e^{-\alpha(1)+4\alpha(\frac{1}{2})+\ln 2 - N(2\alpha(\frac{1}{2})+2\ln 2)+2N_{f_l}\alpha(\frac{1}{2})}}{\pi^2(N-1)!(N-2)!} \left( \frac{\ln \lambda(11N - 2N_f)}{3} \right)^{2N} \times \\ &\times e^{-\frac{8\pi^2}{g^2(N_f, N, 1/\varrho)}} \frac{\prod_f m_f \varrho}{\varrho^5} f(0, \varrho)|_{N_{f_l}, T>0} \prod_{f_h} e^{-p(m_{f_h}, \varrho)} \end{aligned} \quad (3.8)$$

with  $g^2(N_f, N, \frac{1}{\varrho})$  given in (2.9) and  $g^{-2N}$  replaced by the purely  $\lambda$ -dependent term as discussed below (2.11); the light quark masses appear only as factors. Generally, we keep the light and heavy flavors  $N_{f_l}$  and  $N_{f_h}$  unspecified and only fix them to the physical case of  $N_{f_l} = 4$ ,  $N_{f_h} = 1$ ,  $N_f = N_{f_l} + N_{f_h} = 5$  when presenting explicit results.

### Step 3)

We compute the topological susceptibility in the DGA by integration over all HS caloron sizes following (2.13) with our result (3.8) plugged in. Then we take the ratio

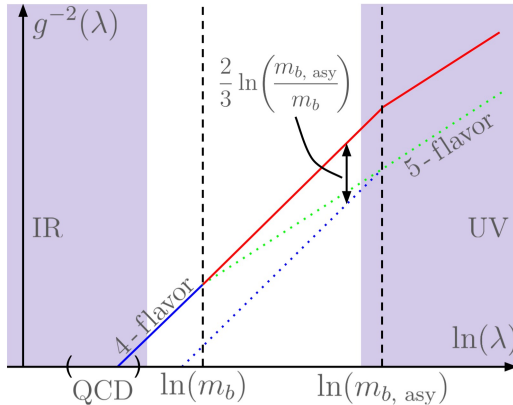


**Figure 2:** The running coupling  $g^{-2}(\lambda)$  for a theory with four light and a heavy  $b$  quark. At large energy scales  $\gg m_b$  one has a 5-flavor running (— · —) which switches to 4-flavor running at the energy scale  $m_b$  (—). For a theory with an asymptotically heavy  $b$  quark, the switch occurs at the UV scale  $m_{b, \text{asy}}$  (· · ·) and the two theories disagree in the IR, with the asymptotic  $b$ -theory failing to describe known 4-flavor QCD/IR theory.

In order to compare the  $m_b$ - and  $m_{b, \text{asy}}$ -theories with matching IR physics, we modify the coupling  $g_{\text{asy}}$  and describe it in terms of  $g_{\text{phys}}$  (3.9) for scales  $> m_b$  (—). Overall,  $g_{\text{asy}}$  is thus given by (— · —). While this description disagrees with the physical description in the UV, it agrees in the IR and thus corresponds better to what happens in a 2 + 1 + 1 flavor lattice calculation.

$\kappa = \frac{\chi_{\text{top}}(m_{f_h}, T)}{\chi_{\text{top}}(m_{f_h, \text{asy}}, T)}$ , comparing a theory with physically heavy quarks to a theory with asymptotically heavy quark masses  $m_{f_h(\text{asy})}$ . Note that  $\kappa \neq \kappa(\lambda)$ .

In order to ensure equal  $N_{f_l}$ -flavor IR theories, we define the running coupling constant (2.9) for the theory containing asymptotically heavy quarks by

$$\frac{8\pi^2}{g_{\text{asy}}^2(N_f, N, 1/\varrho, \lambda)} = \underbrace{\frac{8\pi^2}{g_{\text{phys}}^2(N_f, N, 1/\varrho, \lambda)}}_{-\frac{1}{3} \ln(\lambda\varrho)(11N-3N_f)} + \frac{2}{3} \sum_{f_h} \ln\left(\frac{m_{f_h, \text{asy}}}{m_{f_h}}\right). \quad (3.9)$$

This is illustrated and described in figure 2.

Together with  $\lim_{m_{f_h, \text{asy}} \rightarrow \infty} p(m_{f_h, \text{asy}}, \varrho) = \frac{1}{3} \ln(m_{f_h, \text{asy}} \varrho)$ , the modifier term in (3.9) cancels  $m_{f_h, \text{asy}}$  in the caloron density, so that  $\kappa \neq \kappa(m_{f_h, \text{asy}})$ . We therefore obtain the  $\chi_{\text{top}}$ -ratio

$$\kappa(m_{f_h}, N_{f_l}, N_{f_h}, N) = \frac{\chi_{\text{top}}(N, m_{f_l}, m_{f_h}, g_{\text{phys}})}{\chi_{\text{top}}(N, m_{f_l}, m_{f_h, \text{asy}}, g_{\text{asy}})}. \quad (3.10)$$

## 4 Small Mass – Taylor Expansion

### 4.1 Structure of the Expansion

We now expand  $f_{\text{ferm}}$  for quarks with a non-vanishing (as opposed to (2.8) and (2.11)) but small mass, in order to obtain  $f_{\text{small}}$  in (3.1). As we discussed in section 3, we can perform

a Taylor expansion of the logarithmic determinant ratio (2.18) at finite  $T$ . We use

$$\begin{aligned} \frac{d}{dm^2} \ln \det(-D_-^2 + m^2) &= \frac{d}{dm^2} \text{Tr} \ln(-D_-^2 + m^2) = \\ &= \text{Tr} \left( \frac{1}{-D_-^2 + m^2} \right) = \int^1 d^4x \text{tr} \left\langle x \left| \frac{1}{-D_-^2 + m^2} \right| x \right\rangle \end{aligned} \quad (4.1)$$

with the anti-periodic closed loop or coincident propagator  $\Delta^-(x, x, m^2) = \langle x | \frac{1}{-D_-^2 + m^2} | x \rangle$  for the  $\mathcal{O}(m^2)$ -coefficient. Including higher orders in the Taylor expansion would require convolutions of such propagators and we thus avoid them.

Coincident propagators are naturally divergent and we achieve regularization via point splitting, i.e., by considering “almost closed loop” propagators  $\Delta^-(x', x, m^2)$  from  $x$  to  $x' = x + \varepsilon$ ,  $\varepsilon \rightarrow 0$ . To retain the gauge invariance of  $\gamma_{s, -}$ , we insert an appropriate Wilson line  $\text{P exp} \left( i \int_x^{x'} dz^\mu A_{\text{HS}}^\mu(z) \right) = 1 + i A_{\text{HS}}^\mu(x) \varepsilon^\mu + \frac{1}{2} \left( i \partial^\mu A_{\text{HS}}^\nu|_x - (A_{\text{HS}}^\mu A_{\text{HS}}^\nu)(x) \right) \varepsilon^\mu \varepsilon^\nu + \mathcal{O}(\varepsilon^3)$  into the propagator. Using also (2.11), we find the Taylor expansion up to  $\mathcal{O}(m^2)$ :

$$\begin{aligned} \gamma_{\text{ferm}} &= -\frac{1}{3} \ln(\lambda \varrho) - 2\alpha \left( \frac{1}{2} \right) + \frac{1}{3} (\pi \varrho)^2 - 2A(\pi \varrho) - \\ &\quad - 2m^2 \lim_{\varepsilon \rightarrow 0} \text{Tr} \left( \left\langle x' \left| \frac{1}{-D_-^2} \right| x \right\rangle \text{P exp} \left( i \int_x^{x'} dz^\mu A_{\text{HS}}^\mu(z) \right) - \left\langle x' \left| \frac{1}{-\partial_-^2} \right| x \right\rangle \right). \end{aligned} \quad (4.2)$$

This expansion contains the spacetime integral over all massless, traced, closed loop propagators of the anti-periodic scalar boson in a periodic caloron background. We try to sketch the intricacy of this system in figure 3.

We therefore require the massless anti-periodic scalar propagator in a caloron and the vacuum background. In general, any (anti-)periodic propagator  $\Delta_{(0)}^\pm(x, y, m^2)$  can be obtained from the corresponding aperiodic propagator  $\bar{\Delta}_{(0)}(\bar{x}, \bar{y}, m^2)$  in  $\mathbb{R}^4$  by adding up time copies [5]

$$\Delta_{(0)}^\pm(x, y, m^2) = \sum_{j \in \mathbb{Z}} (\pm 1)^j \bar{\Delta}_{(0)}(\bar{x}, \bar{y} + j \hat{e}_4, m^2) \quad (4.3)$$

(compare the construction of the caloron from instantons). Performing the time-copy sums amounts to compactifying the spacetime in the temporal direction  $\mathbb{R}^4 \rightarrow \mathbb{R}^3 \times S_{\text{rad} = 1/2\pi}^1$ , therefore the bars are dropped:  $\bar{\Delta} \rightarrow \Delta$ ,  $|\vec{\bar{x}}|, |\vec{\bar{y}}| \rightarrow r_x, r_y$ ,  $\bar{t}, \bar{t}_y \rightarrow \tau_x, \tau_y$ , etc.

In the following section 4.2 we obtain this massless closed loop propagator  $\Delta^\pm(x, x')$  in point splitting regularization. In appendix C we derive the traceful parts for general massless propagators  $\Delta^\pm(x, y)$  (the traceless parts can be obtained analogously).

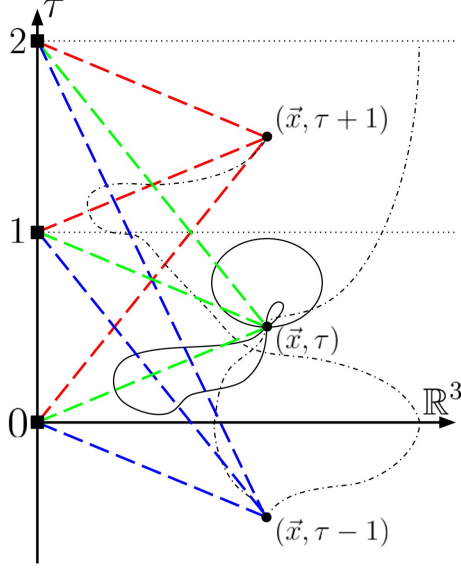


**Figure 3:** Some closed loop-propagators in the periodic spacetime  $\mathbb{R}^3 \times S^1_{\text{rad}=1/2\pi}$  as they appear in (4.2). The periodicity of the spacetime is made explicit by showing all the time copies of the boson and BPST instanton making up the thermal boson and HS caloron, respectively.

The anti-periodic boson copies are located at  $(\bullet) x + j\hat{e}_4$ ,  $j \in \mathbb{Z}$  and are connected by closed loops; the solid lines (—) show “aperiodically closed loops” which do not encounter the spacetime periodicity, the dash-dotted lines (-·-·-) show loops which encounter the periodicity  $j$  times and close (anti-)periodically for  $j$  even (odd). The caloron is made up of periodic instanton copies located at  $(\blacksquare) 0 + j\hat{e}_4$ .

All boson copies and all connecting, closed loop-propagators are affected by all periodic copies of the instanton; this is symbolized by the dashed red, green and blue lines (- - -) connecting the instanton and boson copies.

## 4.2 Massless closed loop scalar Propagator

First, we require the aperiodic  $\mathbb{R}^4$ -propagator for a scalar field in a HS caloron background. An *Ansatz* for this propagator can be found by employing the results of [36]:

$$\bar{\Delta}(\bar{x}, \bar{y}) = \frac{1}{\sqrt{\phi(x)}} \frac{F(\bar{x}, \bar{y})}{4\pi^2(\bar{x} - \bar{y})^2} \frac{1}{\sqrt{\phi(y)}}, \quad (4.4)$$

$$\begin{aligned} F(\bar{x}, \bar{y}) &= 1 + \varrho^2 \sum_{k \in \mathbb{Z}} \frac{\sigma^\mu(\bar{x} - k\hat{e}_4)^\mu \sigma^{\dagger\nu}(\bar{y} - k\hat{e}_4)^\nu}{(\bar{x} - k\hat{e}_4)^2 (\bar{y} - k\hat{e}_4)^2} = \\ &= 1 + \varrho^2 \sum_{k \in \mathbb{Z}} \frac{\vec{\bar{x}} \cdot \vec{\bar{y}} + (\bar{t}_x - k)(\bar{t}_y - k) + i(\bar{t}_x - k)\vec{\bar{y}} \cdot \vec{\sigma} - i(\bar{t}_y - k)\vec{\bar{x}} \cdot \vec{\sigma} + i(\vec{\bar{x}} \times \vec{\bar{y}}) \cdot \vec{\sigma}}{\vec{\bar{x}}^2 \vec{\bar{y}}^2 + \vec{\bar{x}}^2(\bar{t}_y - k)^2 + \vec{\bar{y}}^2(\bar{t}_x - k)^2 + (\bar{t}_x - k)^2(\bar{t}_y - k)^2}. \end{aligned} \quad (4.5)$$

Since  $\phi$  (2.2) is periodic in the  $\bar{t}$ -direction, the  $\bar{x}$ - and  $x$ -coordinates are equivalent. We then plug (4.4) and (4.5) into (4.3).

In order to obtain closed loop-propagators  $\Delta^\pm(x', x)$  from (4.3), we set  $\bar{y} \rightarrow \bar{x}$  and  $\bar{x} \rightarrow \bar{x}' = \bar{x} + \bar{\varepsilon}$  in (4.4) and (4.5). The  $j = 0$ -term in (4.3) then corresponds to the aperiodically closed loops in figure 3, while the  $j \neq 0$ -modes correspond to the anti-periodically closed loops. Thus we can identify the diverging and finite parts of  $\Delta^\pm(x, x')$  corresponding to  $j = 0$ - and  $j \neq 0$ -modes, respectively.

For the finite part of  $\Delta^\pm(x', x)$ , we can safely take the limit  $\bar{\varepsilon} \rightarrow 0$  as  $j \neq 0$ . First, we focus on the traceful part of (4.4), denoted as  $=_{\text{tr}}$ , and calculate (4.5):

$$\begin{aligned} F(\bar{x}, \bar{x} + j \hat{e}_4) &=_{\text{tr}} 1 + \sum_{k \in \mathbb{Z}} \frac{\varrho^2 (\vec{\bar{x}}^2 + (\bar{t} - k)(\bar{t} + j - k))}{\vec{\bar{x}}^4 + \vec{\bar{x}}^2(\bar{t} + j - k)^2 + \vec{\bar{x}}^2(\bar{t} - k)^2 + (\bar{t} - k)^2(\bar{t} + j - k)^2} = \\ &= 1 + \frac{4\pi\varrho^2 |\vec{\bar{x}}| \sinh(2\pi|\vec{\bar{x}}|)}{(4\vec{\bar{x}}^2 + j^2)(\cosh(2\pi|\vec{\bar{x}}|) - \cos(2\pi\bar{t}))}. \end{aligned} \quad (4.6)$$

We can now perform the  $j$ -summation according to (4.3) and find the traceful finite part of the coincident (anti-)periodic propagator:

$$\begin{aligned} \sum_{j \in \mathbb{Z} \setminus \{0\}} (\pm 1)^j \bar{\Delta}(\bar{x}, \bar{x} + j \hat{e}_4) &= \sum_{j \in \mathbb{Z} \setminus \{0\}} \frac{(\pm 1)^j F(\bar{x}, \bar{x} + j \hat{e}_4)}{4\pi^2 j^2 \phi(x)} =_{\text{tr}} \\ &=_{\text{tr}} \sum_{j \in \mathbb{Z} \setminus \{0\}} \frac{(\pm 1)^j}{4\pi^2 \phi(x)} \left( \frac{1}{j^2} + \left( \frac{1}{j^2} - \frac{1}{4\vec{\bar{x}}^2 + j^2} \right) \frac{\pi\varrho^2 \sinh(2\pi|\vec{\bar{x}}|)}{|\vec{\bar{x}}|(\cosh(2\pi|\vec{\bar{x}}|) - \cos(2\pi\bar{t}))} \right) = \\ &= \left\{ \begin{array}{c} + \frac{1}{12} \\ - \frac{1}{24} \end{array} \right\} + \frac{\varrho^2 \sinh(2\pi r)}{16\pi r^3 (\cosh(2\pi r) - \cos(2\pi\tau)) \phi(x)} \left( 1 - 2\pi r \cdot \left\{ \begin{array}{c} \coth(2\pi r) \\ \text{csch}(2\pi r) \end{array} \right\} \right), \end{aligned} \quad (4.7)$$

where we used that  $\frac{1}{j^2(4\vec{\bar{x}}^2 + j^2)} = \frac{1}{4\vec{\bar{x}}^2 j^2} - \frac{1}{4\vec{\bar{x}}^2(4\vec{\bar{x}}^2 + j^2)}$ . We abbreviate  $\{+\frac{1}{12}, -\frac{1}{24}\} = C^\pm$ . This finite contribution contains the corresponding finite contribution to the free propagator

$$\sum_{j \in \mathbb{Z} \setminus \{0\}} (\pm 1)^j \bar{\Delta}_0(\bar{x}, \bar{x} + j \hat{e}_4) = \sum_{j \in \mathbb{Z}} \frac{(\pm 1)^j}{4\pi^2 j^2} = C^\pm, \quad (4.8)$$

which physically represents the well known effect of a mass on the thermal part of the pressure.

Second, we find the finite traceless part of (4.3) to vanish. To see that, we calculate the traceless part of (4.5), denoted as  $=_{\setminus \text{tr}}$ ,

$$\begin{aligned} F(\bar{x}, \bar{x} + j \hat{e}_4) &=_{\setminus \text{tr}} \sum_{k \in \mathbb{Z}} \frac{-i\varrho^2 j \vec{\bar{x}} \cdot \vec{\sigma}}{\vec{\bar{x}}^4 + \vec{\bar{x}}^2(\bar{t} - k)^2 + \vec{\bar{x}}^2(\bar{t} + j - k)^2 + (\bar{t} - k)^2(\bar{t} + j - k)^2} = \\ &= -\frac{2i\pi\varrho^2 \sinh(2\pi|\vec{\bar{x}}|) \hat{e}_{\vec{\bar{x}}} \cdot \vec{\sigma}}{\cosh(2\pi|\vec{\bar{x}}|) - \cos(2\pi\bar{t})} \frac{j}{4\vec{\bar{x}}^2 + j^2} \end{aligned} \quad (4.9)$$

and note that it is odd in  $j$ , i.e., the time copy sums vanish:

$$\sum_{j \in \mathbb{Z} \setminus \{0\}} (\pm 1)^j \bar{\Delta}(\bar{x}, \bar{x} + j \hat{e}_4) \propto_{\setminus \text{tr}} \sum_{j \in \mathbb{Z} \setminus \{0\}} \frac{(\pm 1)^j j}{(4\vec{\bar{x}}^2 + j^2) j^2} = 0. \quad (4.10)$$



Turning to the infinite (or rather, regularized) part of  $\Delta^\pm(x', x)$ , we set  $j = 0$ , but have to keep  $\bar{\varepsilon}$ . We choose a temporal splitting  $\bar{x}' = \bar{x} + \bar{\varepsilon}_\tau \hat{e}_4$ . Note that this procedure for the  $j = 0$ -mode is equivalent for the periodic and anti-periodic case. In temporal point splitting regularization the traceful part of (4.5) reads

$$\begin{aligned}
F(\bar{x}', \bar{x}) &= \text{tr} \\
&= \text{tr} \, 1 + \sum_{k \in \mathbb{Z}} \frac{\varrho^2 (\vec{\bar{x}}^2 + (\bar{t} + \bar{\varepsilon}_\tau - k)(\bar{t} - k))}{\vec{\bar{x}}^4 + \vec{\bar{x}}^2(\bar{t} - k)^2 + \vec{\bar{x}}^2(\bar{t} + \bar{\varepsilon}_\tau - k)^2 + (\bar{t} + \bar{\varepsilon}_\tau - k)^2(\bar{t} - k)^2} = \\
&= 1 + \frac{\pi \varrho^2}{4 \vec{\bar{x}}^2 + \bar{\varepsilon}_\tau^2} \left( 2 |\vec{\bar{x}}| \sinh(4\pi |\vec{\bar{x}}|) - 2 |\vec{\bar{x}}| \sinh(2\pi |\vec{\bar{x}}|) (\cos(2\pi \bar{t}) + \cos(2\pi(\bar{t} + \bar{\varepsilon}_\tau))) - \right. \\
&\quad \left. - \bar{\varepsilon}_\tau \cosh(2\pi |\vec{\bar{x}}|) (\sin(2\pi(\bar{t} + \bar{\varepsilon}_\tau)) - \sin(2\pi \bar{t})) + \bar{\varepsilon}_\tau \sin(2\pi \bar{\varepsilon}_\tau) \right) \times \\
&\quad \times \frac{1}{(\cosh(2\pi |\vec{\bar{x}}|) - \cos(2\pi \bar{t})) (\cosh(2\pi |\vec{\bar{x}}|) - \cos(2\pi(\bar{t} + \bar{\varepsilon}_\tau)))} \tag{4.11}
\end{aligned}$$

and for the traceless part we find

$$\begin{aligned}
F(\bar{x}', \bar{x}) &= \text{tr} \sum_{k \in \mathbb{Z}} \frac{i \varrho^2 \bar{\varepsilon}_\tau \vec{\bar{x}} \cdot \vec{\sigma}}{\vec{\bar{x}}^4 + \vec{\bar{x}}^2(\bar{t} - k)^2 + \vec{\bar{x}}^2(\bar{t} + \bar{\varepsilon}_\tau - k)^2 + (\bar{t} + \bar{\varepsilon}_\tau - k)^2(\bar{t} - k)^2} = \\
&= \frac{i \pi \varrho^2 \vec{\bar{x}} \cdot \vec{\sigma}}{|\vec{\bar{x}}| (4 \vec{\bar{x}}^2 + \bar{\varepsilon}_\tau^2)} \left( \bar{\varepsilon}_\tau \sinh(4\pi |\vec{\bar{x}}|) + 2 |\vec{\bar{x}}| \cosh(2\pi |\vec{\bar{x}}|) (\sin(2\pi(\bar{t} + \bar{\varepsilon}_\tau)) - \sin(2\pi \bar{t})) - \right. \\
&\quad \left. - \bar{\varepsilon}_\tau \sinh(2\pi |\vec{\bar{x}}|) (\cos(2\pi \bar{t}) + \cos(2\pi(\bar{t} + \bar{\varepsilon}_\tau))) - 2 |\vec{\bar{x}}| \sin(2\pi \bar{\varepsilon}_\tau) \right) \times \\
&\quad \times \frac{1}{(\cosh(2\pi |\vec{\bar{x}}|) - \cos(2\pi \bar{t})) (\cosh(2\pi |\vec{\bar{x}}|) - \cos(2\pi(\bar{t} + \bar{\varepsilon}_\tau)))}. \tag{4.12}
\end{aligned}$$

Multiplied by  $(\phi(x')\phi(x))^{-1/2}$ , (4.11) and (4.12) give the traceful and traceless  $j = 0$ -contributions to (4.3), respectively.

By plugging (4.7) - (4.12) into (4.3) we find the massless periodic and anti-periodic coincident propagator at finite temperature, regularized via point splitting in the temporal direction. Finally, we perform a Taylor expansion in  $\bar{\varepsilon}_\tau$ :

$$\begin{aligned}
\Delta^\pm(x' = x + \varepsilon_\tau \hat{e}_4, x) &= \frac{F(\bar{x}', \bar{x})}{4\pi^2 \bar{\varepsilon}_\tau^2 \sqrt{\phi(x')\phi(x)}} + \sum_{j \in \mathbb{Z} \setminus \{0\}} \frac{(\pm 1)^j F(\bar{x}, \bar{x} + j \hat{e}_4)}{4\pi^2 j^2 \phi(x)} = \\
&= \frac{1}{4\pi^2 \varepsilon_\tau^2} + C^\pm + \frac{\varrho^2 \sinh(2\pi r) \left( 1 - 2\pi r \cdot \left\{ \begin{array}{l} \coth(2\pi r) \\ \text{csch}(2\pi r) \end{array} \right\} \right)}{16\pi r^3 (\cosh(2\pi r) - \cos(2\pi \tau)) \phi(x)} - \\
&\quad - \frac{\varrho^2}{64\pi r^3} \left[ \sinh(6\pi r) + 4\pi r \cosh(4\pi r) \cos(2\pi \tau) - \right. \\
&\quad \left. - \sinh(2\pi r) \left( \frac{8\pi^3 \varrho^2 r \sinh(2\pi r) \sin^2(2\pi \tau)}{(\cosh(2\pi r) - \cos(2\pi \tau)) \phi(x)} - 2 \cos(2\pi \tau) - 3 \right) - \right.
\end{aligned}$$

$$\begin{aligned}
& - 4(\sinh(4\pi r) - 3\pi r) \cos(2\pi\tau) - 4\pi r \cosh(2\pi r)(\cos(4\pi\tau) + 3) \Big] \times \\
& \times \left( (\cosh(2\pi r) - \cos(2\pi\tau))^3 \phi(x) \right)^{-1} + \\
& + \frac{i\varrho^2 \sigma^r}{64\pi r^3 \varepsilon_\tau} \left[ r \sinh(8\pi r) + \pi \varrho^2 \cosh(8\pi r) + ((4\pi^2 \varrho^2 - 6)r \sinh(6\pi r) + \right. \\
& + 4\pi(r^2 - \varrho^2) \cosh(6\pi r)) \cos(2\pi\tau) - 2\pi((4r^2 - \varrho^2)(2 + \cos(4\pi\tau)) + \varrho^2) \cosh(4\pi r) - \\
& - 12\pi^2 \varrho^2 r \sinh(4\pi r) + 8r \sinh(4\pi r) - 2(2\pi^2 \varrho^2 - 3)r \sinh(4\pi r) \cos(4\pi\tau) + \\
& + 4\pi \cosh(2\pi r)((14r^2 + \varrho^2) \cos(2\pi\tau) + r^2 \cos(6\pi\tau)) - 2r \sinh(2\pi r) \cos(6\pi\tau) + \\
& \left. + 4(5\pi^2 \varrho^2 - 3)r \sinh(2\pi r) \cos(2\pi\tau) - \pi(8r^2 + \varrho^2)(2 \cos(4\pi\tau) + 3) \right] \times \\
& \times \left( (\cosh(2\pi r) - \cos(2\pi\tau))^4 \phi^2(x) \right)^{-1} - \\
& - \frac{i\varrho^2 \sigma^r}{64\pi r^3} \left[ 2\pi r(2\pi r \cosh(6\pi r) + 8\pi^2 \varrho^2 \sinh^3(2\pi r) + \sinh(6\pi r)) \sin(2\pi\tau) - \right. \\
& - 4\pi r \sinh(4\pi r) - 4\pi^2 r^2 \cosh(2\pi r)(6 \sin(2\pi\tau) + \sin(6\pi\tau)) + \\
& \left. + 2\pi r \sinh(2\pi r)(2 \sin(4\pi\tau) + \sin(6\pi\tau)) + 16\pi^2 r^2 \sin(4\pi\tau) \right] \times \\
& \times \left( (\cosh(2\pi r) - \cos(2\pi\tau))^4 \phi^2(x) \right)^{-1} + \mathcal{O}(\varepsilon_\tau) \tag{4.13}
\end{aligned}$$

with  $C^\pm = \{\frac{1}{12}, -\frac{1}{24}\}$ , and  $\sigma^r = \begin{pmatrix} \cos(\theta) & \sin(\theta)e^{-i\varphi} \\ \sin(\theta)e^{i\varphi} & -\cos(\theta) \end{pmatrix}$  being a function of only the polar and azimuthal angles  $\theta, \varphi$ . Note also:  $\text{tr}(\sigma^r) = 0$  and  $(\sigma^r)^2 = 1$ .

The first two (constant) diagonal terms in  $\Delta^\pm(x', x)$  correspond to the periodic/anti-periodic free field coincident propagator  $\Delta_0^\pm(x', x) = \Delta^\pm(x', x)|_{\varrho=0} = \frac{1}{4\pi^2 \varepsilon_\tau^2} + C^\pm$ . The spacetime-dependent diagonal terms (third and fourth term) we write as  $\Delta_{\text{diag, finite}}^\pm(x)$ . In the periodic case, this finite contribution vanishes polynomially as  $\Delta_{\text{diag, finite}}^+ \stackrel{r \rightarrow \infty}{\propto} -\frac{\varrho^2}{8r^2}$  for large distances from the caloron, while for the anti-periodic scalar of interest this term falls off exponentially as  $\Delta_{\text{diag, finite}}^- \stackrel{r \rightarrow \infty}{\propto} -\frac{\varrho^2}{2r^2} e^{-2\pi r} \cos^2(\pi\tau)$ . The off-diagonal part of the coincident propagator (fifth and sixth term) contains an “ $\varepsilon_\tau \rightarrow 0$ -diverging” term and a finite one, which we denote as  $i\sigma^r(x) \varepsilon_\tau^{-1} \Delta_{\text{off-diag, infinite}}(x)$  and  $i\sigma^r(x) \Delta_{\text{off-diag, finite}}(x)$ . They fall off as  $\Delta_{\text{off-diag, infinite}} \stackrel{r \rightarrow \infty}{\propto} \frac{\varrho^2}{8\pi r^2}$  and  $\Delta_{\text{off-diag, finite}} \stackrel{r \rightarrow \infty}{\propto} -\frac{\pi \varrho^2}{2r} e^{-2\pi r} \sin(2\pi\tau)$ .

The fact that the anti-periodic propagator falls off exponentially at large separation, but the periodic one does not, explains why it is possible to perform an  $m^2$ -expansion in the anti-periodic but not the periodic case. For periodic boundary conditions, the lowest Matsubara frequency is zero, and the logarithmic IR effects present in vacuum become more severe, appearing as a linear divergence in the  $m^2$ -coefficient. We expect that the true  $m^2$ -dependence will be non-analytic  $\propto m$ , similar to what happens in the finite- $m$  expansion of the pressure [45].

For small distances from the caloron (center) the coincident propagator - terms scale as  $\Delta_{\text{diag, finite}}^+ \stackrel{r \rightarrow 0}{\propto} -\frac{\pi^2 \varrho^2 (1 + \pi^2 \varrho^2)}{2(2\pi^2 \varrho^2 + 1 - \cos(2\pi\tau))^2}$ ,  $\Delta_{\text{diag, finite}}^- \stackrel{r \rightarrow 0}{\propto} -\frac{\pi^2 \varrho^2 \cos^2(\pi\tau)}{2(2\pi^2 \varrho^2 + 1 - \cos(2\pi\tau))^2}$  for the periodic and anti-periodic traceful terms and  $\Delta_{\text{off-diag, infinite}} \stackrel{r \rightarrow 0}{\propto} r \frac{\pi^2 \varrho^2 (2 + \cos(2\pi\tau)) \csc^2(\pi\tau)}{6(2\pi^2 \varrho^2 + 1 - \cos(2\pi\tau))}$  and  $\Delta_{\text{off-diag, finite}} \stackrel{r \rightarrow 0}{\propto} -r \frac{\pi^3 \varrho^2 (12\pi^2 \varrho^2 + 9 - 8 \cos(2\pi\tau) - \cos(4\pi\tau)) \cot(\pi\tau) \csc^2(\pi\tau)}{12(2\pi^2 \varrho^2 + 1 - \cos(2\pi\tau))^2}$  for the traceless parts.

Using all of the above abbreviations, we write the closed loop propagator (4.13) as

$$\begin{aligned} \Delta^\pm(x', x) &= \frac{1}{4\pi^2 \varepsilon_\tau^2} + C^\pm + \Delta_{\text{diag, finite}}^\pm(r, \tau) + \frac{i\sigma^r}{\varepsilon_\tau} \Delta_{\text{off-diag, infinite}}(r, \tau) + \\ &+ i\sigma^r \Delta_{\text{off-diag, finite}}(r, \tau) + \mathcal{O}(\varepsilon_\tau). \end{aligned} \quad (4.14)$$

### 4.3 Taylor Expansion – Numerical Results

We can now plug (4.14) into (4.2). According to the temporal point splitting employed for the coincident propagator, we also have to include a temporal Wilson line from  $x$  to  $x'$  in (4.2). Using  $A_{\text{HS}}^4 = -\bar{\eta}^{a4\nu} \partial^\nu \ln(\phi(r, \tau)) \frac{\sigma^a}{2} = -\vec{\partial} \ln \phi \cdot \frac{\vec{\sigma}}{2} = -\frac{\partial_r \phi}{\phi} \frac{\sigma^r}{2}$  we find the Wilson line

$$\begin{aligned} e^{i \int_\tau^{\tau+\varepsilon_\tau} d\tau A_{\text{HS}}^4(\vec{x}, \tau)} &= 1 + i A_{\text{HS}}^4(x) \varepsilon_\tau + \frac{1}{2} \left( i \partial_\tau A_{\text{HS}}^4|_x - (A_{\text{HS}}^4(x))^2 \right) \varepsilon_\tau^2 + \mathcal{O}(\varepsilon_\tau^3) = \\ &= 1 - \frac{1}{8} \left( \frac{\partial_r \phi}{\phi} \Big|_x \right)^2 \varepsilon_\tau^2 - i \frac{\sigma^r}{2} \left( \frac{\partial_r \phi}{\phi} \varepsilon_\tau + \frac{\partial_\tau \partial_r \phi}{2\phi} \varepsilon_\tau^2 - \frac{\partial_\tau \phi \partial_r \phi}{2\phi^2} \varepsilon_\tau^2 \right) \Big|_x + \mathcal{O}(\varepsilon_\tau^3). \end{aligned} \quad (4.15)$$

We note the large- and small- distance behavior of the caloron field  $A_{\text{HS}}^4 \propto \frac{\partial_r \phi}{\phi} \stackrel{r \rightarrow \infty}{\propto} -\frac{\pi \varrho^2}{r^2}$  and  $\frac{\partial_r \phi}{\phi} \stackrel{r \rightarrow 0}{\propto} -r \frac{8\pi^4 \varrho^2 (2 + \cos(2\pi\tau))}{3(2\pi^2 \varrho^2 + 1 - \cos(2\pi\tau))(1 - \cos(2\pi\tau))}$ .

Plugging now also (4.15) into (4.2), we find the  $m^2$ -coefficient  $-2\gamma_{s, -}^{\text{small}}$  of the  $\gamma_{\text{ferm}} -$  expansion (3.2):

$$\begin{aligned} -2\gamma_{s, -}^{\text{small}}(\varrho) &= -2 \lim_{\varepsilon_\tau \rightarrow 0} \text{Tr} \left( \frac{1}{4\pi^2 \varepsilon_\tau^2} + C^- - \frac{1}{32\pi^2} \left( \frac{\partial_r \phi}{\phi} \Big|_x \right)^2 + \Delta_{\text{diag, finite}}^-(r, \tau) + \right. \\ &\quad \left. + \frac{1}{2} \Delta_{\text{off-diag, infinite}}(r, \tau) \frac{\partial_r \phi}{\phi} \Big|_x + \mathcal{O}(\varepsilon_\tau) - \Delta_0^-(x', x) \right) = \\ &= -2 \int_0^1 d\tau \int_0^\infty dr r^2 \left( -\frac{1}{4\pi} \left( \frac{\partial_r \phi}{\phi} \Big|_x \right)^2 + 8\pi \Delta_{\text{diag, finite}}^-(r, \tau) + \right. \\ &\quad \left. + 4\pi \Delta_{\text{off-diag, infinite}}(r, \tau) \frac{\partial_r \phi}{\phi} \Big|_x \right), \end{aligned} \quad (4.16)$$

where the factor  $8\pi$  in the second step is due to the solid angle integration and taking the  $\mathfrak{su}(2)$ -trace.

Due to the aforementioned large- and small- distance behavior of  $\frac{\partial_r \phi}{\phi}$ ,  $\Delta_{\text{diag, finite}}^+$ , and  $\Delta_{\text{off-diag, infinite}}^+$ , the integral  $\gamma_{s, -}^{\text{small}}$  is finite and we can calculate it numerically for different values of the parameter  $\varrho$ . It is of interest to note that in the periodic case the corresponding integral  $\gamma_{s, +}$  is linearly divergent. This is due to  $\Delta_{\text{diag, finite}}^+(r, \tau)$  scaling as  $r^{-2}$  for large distances as we stated above.

We obtain  $\gamma_{s,-}^{\text{small}}$  by numerical integration for a range of logarithmically spaced caloron sizes  $5 \cdot 10^{-4} \leq \varrho < 135$ ; it is well described by the following approximate form (we include the values and error of the fitting function in the ancillary files):

$$\gamma_{s,-}^{\text{small}}(\varrho) = \begin{cases} -0.5\tilde{\varrho}^2 \ln(0.946\tilde{\varrho}) & 0 \leq \varrho \leq 0.082 \\ -0.85\varrho^{1.80} + 0.59\varrho^{1.28} & 0.082 < \varrho \leq 1.045 \\ -0.76\varrho^2 & 1.045 < \varrho \end{cases} \quad (4.17)$$

We have divided  $\varrho$  into three regions; a small region where the heavy quark effect is approximately the same as for a zero-temperature instanton (described by  $\tilde{\varrho}$ ); an intermediate region which is of the most physical interest; and a large region where thermal effects grow with caloron size as  $\varrho^2$ . We display the numerical values for  $\gamma_{s,-}^{\text{small}}(\varrho)$  in [figure 4](#).

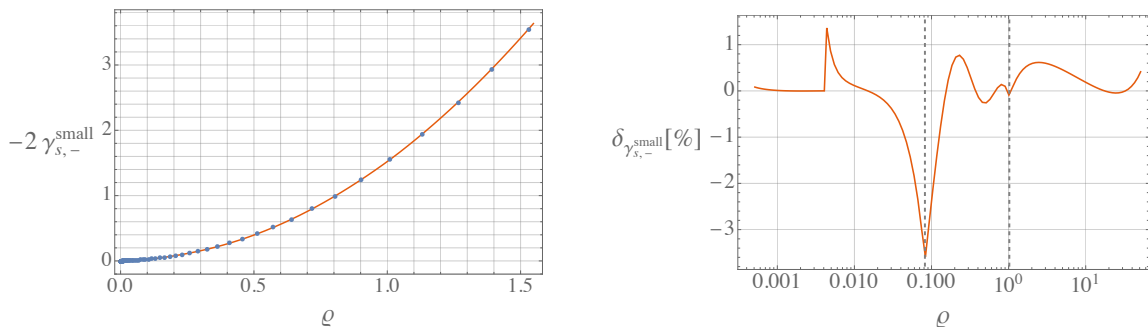


**Figure 4:** Left:  $m^2$  coefficient  $-2\gamma_{s,-}^{\text{small}}$  as a function of the caloron size  $\varrho$ . Right: percent relative error of our fitting function, (4.17). For the physically most important region  $0.2 < \varrho < 0.6$ , the fit is accurate to better than 1%.

Our final small-mass result for the fermionic correction factor (3.1), using (4.2) together with (4.17), reads:

$$f_{\text{small}}(m, \varrho) = f(0, \varrho)|_{T > 0, \text{ ferm}} e^{2m^2\gamma_{s,-}^{\text{small}}(\varrho)} = \exp\left(-\frac{(\pi\varrho)^2}{3} + 2A(\pi\varrho) + 2m^2\gamma_{s,-}^{\text{small}}(\varrho)\right). \quad (4.18)$$

The small-mass expansion is reasonable where  $\gamma_{s,-}^{\text{small}}(\varrho)$  itself is small, which unsurprisingly is when  $m < \varrho^{-1}$ . We add the condition that  $m < 1$ , as otherwise the small-mass expansion of the thermal part of the pressure is also not under control. For the physically most important region around  $\varrho \sim 0.4$ , this latter condition is stronger.

## 5 Large Mass – Heat Kernel Expansion

### 5.1 Structure of the Expansion

In order to perform the large-mass ( $m \gg 1$ )-expansion, we proceed analogously to [41] and employ the *Schwinger proper time* ( $s$ ) representation of the logarithmic correction factor term (2.18). In this representation the mass is again (like for the Taylor expansion) separated from the purely caloron-dependent differential operator  $-D_-^2$  and from  $-\partial_-^2$ :

$$\gamma_{s,-} = -\int_0^\infty \frac{ds}{s} (e^{-m^2s} - e^{-\lambda^2s}) \text{Tr} \left( \langle x | (e^{-(D_-^2)s} - e^{-(\partial_-^2)s}) | x \rangle \right). \quad (5.1)$$

The proper time  $s$  is also  $\beta^{-2}$ -rescaled with  $[s] = \text{mass}^{-2}$ .  $\langle x | e^{-(D_-^2)s} | y \rangle = \langle xs | y \rangle^-$  and  $\langle x | e^{-(\partial_-^2)s} | y \rangle = \langle xs | y \rangle_0^-$  are the anti-periodic proper time-Green's functions, i.e., they satisfy proper time-Schrödinger equations:  $-\partial_s \langle xs | y \rangle^- = -D_{x,-}^2 \langle xs | y \rangle^-$  and analogously for  $\langle xs | y \rangle_0^-$ . These Green's functions describe a propagation from  $y$  to  $x$  in proper time  $s$ . The ordinary anti-periodic propagators from  $y$  to  $x$  in Euclidean time are then reproduced by  $s$ -integration:

$$\Delta^-(x, y, m^2) = \left\langle x \left| \frac{1}{-D_-^2 + m^2} \right| y \right\rangle = \int_0^\infty ds \langle xs | y \rangle^- e^{-m^2 s} \quad (5.2)$$

and analogously for  $\Delta_0^-(x, y, m^2)$  [46]. Since the ordinary propagator  $[\Delta_{(0)}^\pm] = \text{mass}^2$  and the  $s$ -integration adds  $[ds] = \text{mass}^{-2}$ , the proper time-Green's functions must be  $[\langle xs | y \rangle_{(0)}^\pm] = \text{mass}^4$ . Their integration with  $[d^4x] = \text{mass}^{-4}$  then yields a dimensionless quantity. As the proper time representation splits off the mass, we can consider the proper time Green's functions of massless, anti-periodic bosons in a caloron background. Thus, the logarithm (5.1) is again given by the spacetime integral over all massless and traced closed loops with a caloron background as shown in figure 3.

The proper time Green's functions are also called the *heat kernels* of their respective operators, here of  $-D_-^2$  and  $-\partial_-^2$ , with respect to proper time and the coincident heat kernels in (5.1) naturally diverge. Regularization is achieved by performing an asymptotic expansion (as mentioned in section 3), the so-called *heat kernel expansion* [47–50]. This expansion is achieved by expanding (5.1) for  $s \lesssim m^{-2} \ll 1$ , which is enforced by the exponential damping  $e^{-m^2 s}$ ,  $m \gg 1$  for non-infinitesimal  $s$ :

$$\text{Tr}(\langle xs | x \rangle^-) = \text{Tr} \left( \left\langle x \left| e^{-(D_-^2)s} \right| x \right\rangle \right) \stackrel{s \searrow 0}{\cong} \sum_{k \in \mathbb{N} \cup \mathbb{N} + \frac{1}{2}} \frac{s^{k-2}}{(4\pi)^2} \int^1 d^4x \text{tr}(b_{2k}(A_{\text{HS}})) \quad (5.3)$$

with the finite- $T$  *heat kernel* or *Seeley-DeWitt coefficients*  $[b_{2k}] = \text{mass}^{2k}$  given in [49, 50].

The large-mass expansion corresponds to inserting the series expansion (5.3) in (5.1), switching the order of the  $k$ -sum and  $s$ -integral, and performing the  $s$ -integral followed by the trace including a spacetime integral. The uniform convergence properties needed to exchange sum and integral are not generally fulfilled, so the large-mass  $k$ -summation is generally only asymptotic. This is actually expected; the identical sum arises for the case of an anti-periodic Klein-Gordon operator  $D_-^2$  as for a periodic one  $D_+^2$ , but the complete result should differ for the two cases. The boundary condition is only expected to matter through terms of order  $m^b e^{-m}$ ,  $b \sim 1$ , which is the typical level of ambiguity associated with summing such an asymptotic series. In using this large-mass series, we must either take care that  $m$  is large enough to allow us to neglect such exponentially small effects, or we must incorporate some other boundary condition-dependent effects. Later we will do so by combining this series with the small- $m^2$  series, which knows explicitly about the boundary conditions. We will also return to the explicit treatment of boundary condition-dependent  $m^b e^{-m}$  effects in appendix B.

The exponential damping of boundary-condition dependence is due to heavy quarks  $m \gg 1$  exploring  $\mathbb{R}^3 \times S_{\text{rad}=1/2\pi}^1$  on length scales  $m^{-1} \ll 1$ , i.e., essentially as they would  $\mathbb{R}^4$ . Figure 5 sketches this: a typical caloron  $\varrho \approx 0.5$  (gray) and the heavy quark-propagation range (red). Temperature only enters in the way that it modifies the caloron fields; the short-range propagation only feels the boundary conditions in an exponentially suppressed fashion because propagation of a heavy field over a distance  $\beta$  is exponentially small.

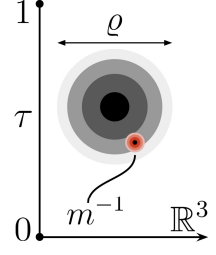


Figure 5

The  $m^{-(2k-4)}$ -expansion at finite temperature is due to the  $T = 0$ -heat kernel coefficients  $\bar{b}_{2k=\text{even}}(A_{\text{HS}}) \subset b_{2k}$  (we discuss the full  $b_{2k}$ -coefficients for  $T > 0$  in appendix B). The  $T = 0$ -heat kernel coefficients are given in [48, 51]:

$$\begin{aligned}
\bar{b}_0 &= 1, \quad \bar{b}_2(\bar{x}) = 0, \quad \bar{b}_4(\bar{x}) = -\frac{1}{12}G^{\mu\nu}G^{\mu\nu}, \quad \bar{b}_6 = \frac{i}{90}G^{\mu\nu}G^{\mu\kappa}G^{\nu\kappa}, \\
\bar{b}_8 &= \frac{17}{210}G^{\mu\nu}G^{\mu\nu}G^{\kappa\lambda}G^{\kappa\lambda} + \frac{2}{35}G^{\mu\nu}G^{\mu\kappa}G^{\nu\lambda}G^{\kappa\lambda} + \frac{1}{105}G^{\mu\nu}G^{\nu\kappa}G^{\kappa\lambda}G^{\lambda\mu} + \\
&\quad + \frac{1}{420}G^{\mu\nu}G^{\kappa\lambda}G^{\mu\nu}G^{\kappa\lambda}, \\
\bar{b}_{10} &= \frac{i}{945}G^{\mu\nu}G^{\kappa\lambda}G^{\alpha\mu}G^{\nu\kappa}G^{\lambda\alpha} - \frac{47i}{126}G^{\mu\nu}G^{\mu\nu}G^{\kappa\lambda}G^{\lambda\alpha}G^{\alpha\kappa} + \\
&\quad + \frac{i}{126}G^{\mu\nu}G^{\kappa\lambda}G^{\mu\nu}G^{\lambda\alpha}G^{\alpha\kappa} + \frac{i}{63}G^{\mu\nu}G^{\nu\kappa}G^{\mu\lambda}G^{\lambda\alpha}G^{\alpha\kappa} - \frac{11i}{189}G^{\mu\nu}G^{\kappa\lambda}G^{\lambda\nu}G^{\mu\alpha}G^{\alpha\kappa} + \\
&\quad + \frac{37i}{945}G^{\mu\nu}G^{\nu\kappa}G^{\kappa\lambda}G^{\lambda\alpha}G^{\alpha\mu} + \frac{4}{189}G^{\nu\alpha}G^{\alpha\lambda}G^{\nu\kappa;\mu}G^{\kappa\lambda;\mu} - \frac{2}{63}G^{\kappa\lambda}G^{\nu\alpha;\mu}G^{\nu\alpha}G^{\kappa\lambda;\mu} - \\
&\quad - \frac{2}{189}G^{\kappa\lambda}G^{\nu\alpha;\mu}G^{\alpha\lambda}G^{\nu\kappa;\mu} + \frac{4}{63}G^{\kappa\lambda}G^{\kappa\lambda}G^{\nu\alpha;\mu}G^{\nu\alpha;\mu} + \frac{2}{63}G^{\mu\kappa}G^{\kappa\lambda}G^{\nu\alpha;\mu}G^{\nu\alpha;\lambda} + \\
&\quad + \frac{4}{189}G^{\kappa\lambda}G^{\lambda\nu}G^{\nu\alpha;\mu}G^{\alpha\kappa;\mu};
\end{aligned} \tag{5.4}$$

$\bar{b}_{12}$  is given in [51, 52] and the  $\bar{b}_{2k>12}$  are unknown. The vacuum coefficient is given by  $\bar{b}_0$ .

## 5.2 Heat Kernel Expansion Order by Order – Numerical Results

Now we plug the heat kernel coefficients (5.4), together with the caloron field strength (derivatives) derived and from (2.1), into (5.1) and (5.3)

$$\gamma_{s,-} = - \int_0^\infty \frac{ds}{s} (e^{-m^2s} - e^{-\lambda^2s}) \int^1 d^4x \operatorname{tr} \left( \sum_{k \in \mathbb{N}} \frac{s^{k-2}}{(4\pi)^2} \bar{b}_{2k}(A_{\text{HS}}(x)) - \bar{b}_{\text{free}} \right), \tag{5.5}$$

performing the  $s$ -integrals first. They are of the structure (analogously for  $\lambda^2$ )

$$I(m^2, k) = \int_0^\infty ds e^{-m^2s} s^{k-3} \begin{cases} \rightarrow \infty & : k \in \{0, 1, 2\} \\ = \frac{1}{m^{2k-4}} \Gamma(k-2) = \frac{(k-3)!}{m^{2k-4}} & : \mathbb{N} \ni k \geq 3 \end{cases}. \tag{5.6}$$

To parametrize the divergences in (5.6), one introduces a small-scale cut-off  $\varepsilon_s$  for the  $s$ -integral and finds

$$\begin{aligned}
I(m^2, 0 \leq k \leq 2) &= \lim_{\varepsilon_s \rightarrow 0} \int_{\varepsilon_s}^{\infty} ds e^{-m^2 s} s^{k-3} = \\
&= \begin{cases} \frac{e^{-m^2 \varepsilon_s} (1 - m^2 \varepsilon_s)}{2\varepsilon_s^2} + \frac{m^4}{2} (\ln(m^2 \varepsilon_s) + \gamma_E + \mathcal{O}(m^2 \varepsilon_s)) & : k = 0 \\ \frac{e^{-m^2 \varepsilon_s}}{\varepsilon_s} + m^2 (\ln(m^2 \varepsilon_s) + \gamma_E + \mathcal{O}(m^2 \varepsilon_s)) & : k = 1 \\ \lim_{\varepsilon_s \searrow 0} \Gamma(0, m^2 \varepsilon_s) = -\ln(m^2 \varepsilon_s) - \gamma_E + \mathcal{O}(m^2 \varepsilon_s) & : k = 2 \end{cases} \quad (5.7)
\end{aligned}$$

where  $\Gamma(0, z)$  is the upper incomplete gamma function.

In the following we consider the different orders of the heat kernel expansion and present our results for the numerical calculation of the resulting caloron density contributions. We obtain explicit functional forms (for numerical  $x$ -integration) for the  $\text{tr}(\bar{b}_{2k})$  by performing analytical calculations using the *OGRe*-package [53] for *Mathematica*.

**Order  $k = 0$ :**

The  $k = 0$ -coefficients of the caloron is  $\bar{b}_0(A_{\text{HS}}) = 1$  and multiplies both the quadratically divergent  $s$ -integral  $I(m^2, 0)$  (5.7) and  $V = \text{vol}(\mathbb{R}^3 \times S_{\text{rad}=1/2\pi}^1) = \int^1 dx^4$ . This contribution is cancelled identically by the free term  $b_{\text{free}} = 1$ . The  $k = 0$ -contribution to  $\gamma_{s, -}$  (5.5) thus vanishes:  $\gamma_0 = 0$ .

**Order  $k = 1$ :**

For  $-D_-^2(A_{\text{HS}})$  the coefficient  $b_2$  vanishes.

**Order  $k = 2$ :**

The  $k = 2$ -proper time integral diverges logarithmically as  $I(m^2, 2) \propto \Gamma(0)$  (5.7); this logarithmic divergence is canceled by the Pauli-Villars -regulator term (see [41, 46] for  $T = 0$ -case). The  $\gamma_E$ -terms of (5.7) cancel as well. The  $\gamma_{s, -}$ -contribution at order  $k = 2$  thus reads

$$\gamma_4(m, \lambda) = \ln\left(\frac{\lambda^2}{m^2}\right) \frac{1}{(4\pi)^2} \text{Tr}(\bar{b}_4) = \ln\left(\frac{m}{\lambda}\right) \frac{1}{6(4\pi)^2} \int^1 d^4x \text{tr}(G^{\mu\nu} G^{\mu\nu}) = \frac{1}{6} \ln\left(\frac{m}{\lambda}\right), \quad (5.8)$$

where we used the definition of the caloron topological charge density (1.1) (analogously to  $T = 0$ -case in [41]).

In order to verify our numerical methods, we compute  $\frac{1}{(4\pi)^2} \text{Tr}(\bar{b}_4(A_{\text{HS}}))$  numerically for 35 caloron sizes ranging over several orders of magnitude from 0.005 to 4854. Our numerical results agree with the analytical value up to corrections which remain below  $2 \times 10^{-7}$  (see our data in the ancillary files) which verifies the precision of our numerical approach.

**Order  $k = 3$ :**

$I(m^2, k)$  is finite for  $k \geq 3$  (5.6), e.g.,  $I(m^2, 3) = \frac{1}{m^2}$ . For  $k = 3$  we find the  $\gamma_s, -$  - term

$$\frac{\gamma_6(\varrho)}{m^2} = I(m^2, 3, 0; 0) \frac{1}{(4\pi)^2} \text{Tr}(\bar{b}_6) = -\frac{1}{1440\pi m^2} \int_0^1 d\tau \int_0^\infty dr r^2 \varepsilon^{abc} G^{a\mu\nu} G^{b\mu\kappa} G^{c\nu\kappa}. \quad (5.9)$$

The corresponding  $\lambda$ -term therefore vanishes as  $\lambda \rightarrow \infty$ . We calculate  $\gamma_6$  for log-spaced  $\varrho$ -values between 0.001 and 477 and describe the results with a fitting function defined piecewise in the regions of small, intermediate, and large caloron sizes:

$$\frac{\gamma_6(\varrho)}{m^2} = \begin{cases} \frac{0.013}{\tilde{\varrho}^{2.00} m^2} & : 0 < \varrho \leq 0.267 \\ \frac{0.128 \tilde{\varrho}^{1.55}}{m^2} + \frac{0.021}{\varrho^{1.78} m^2} & : 0.267 < \varrho \leq 1.844 . \\ \frac{0.008}{\varrho^{2.00} m^2} + \frac{0.052}{m^2} & : 1.844 < \varrho \end{cases} \quad (5.10)$$

This fit agrees with the exact numerical integration to within (about) 0.3% across all

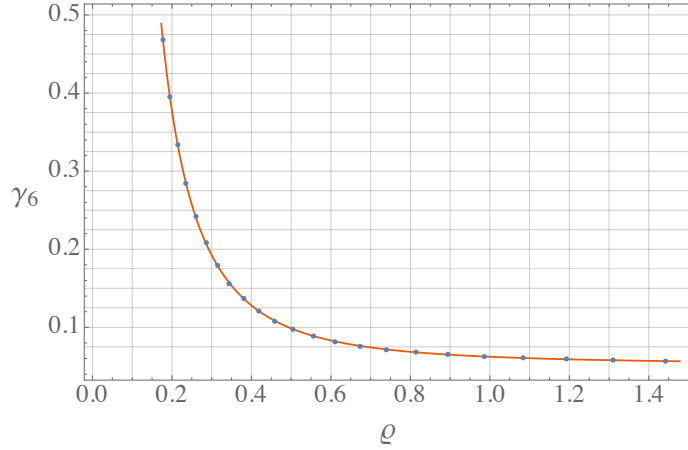


**Figure 6:** Numerical result for  $\gamma_6(\varrho)$ , the  $m^{-2}$ -coefficient, as a function of caloron size  $\varrho$ .

caloron sizes. Note that the  $\varrho \ll 1$  regime agrees with the exact result in an instanton background,  $\gamma_6(\varrho) = 1/(75\varrho^2) = 0.01\bar{3}/\varrho^2$ . We show the result of the numerical integration in figure 6 and provide a table of the numerical values as a function of  $\varrho$  and the fitting error in the ancillary files.



**Order  $k = 4$ :**

Using (5.6) with  $I(m^2, 4, 0; 0) = \frac{1}{m^4}$ , we calculate the  $\gamma_{s, -}$ -contribution at  $k = 4$  for log-spaced caloron sizes between 0.001 and 462:

$$\begin{aligned} \frac{\gamma_8(\varrho)}{m^4} &= I(m^2, 4, 0; 0) \frac{1}{(4\pi)^2} \text{Tr}(\bar{b}_8) = \\ &= \begin{cases} \frac{0.023}{\tilde{\varrho}^4 m^4} & : 0 < \varrho \leq 0.120 \\ \frac{0.090}{\tilde{\varrho}^{2.34} m^4} + \frac{0.021}{\varrho^{4.03} m^4} & : 0.120 < \varrho \leq 1.183, \\ \frac{0.020}{\varrho^{3.11} m^4} + \frac{0.096}{\varrho^{1.99} m^4} + \frac{0.388}{m^4} & : 1.183 < \varrho \end{cases} \end{aligned} \quad (5.11)$$

where the full  $\varrho < 0.12$ -coefficient in (5.11) fits the expected instanton  $m^{-4}$ -coefficient  $\frac{17}{735}$  in [41] up to 1%. The fitting function is generally accurate to about 1% except around  $\varrho = 0.25$ , where it deviates from the numerical results by up to circa 3%. Again, the numerical results are tabulated in the ancillary files. The result of numerical integration is presented in figure 7.

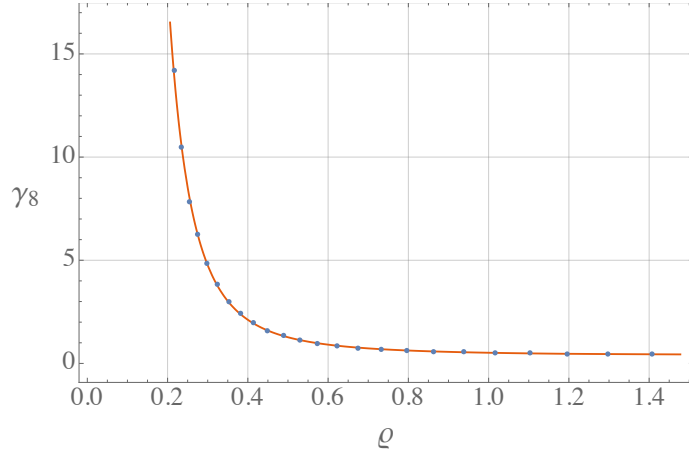


**Figure 7:** Coefficient  $\gamma_8(\varrho)$ , describing  $m^{-4}$  corrections, as a function of caloron size  $\varrho$ .

**Order  $k = 5$ :**

We calculate the  $\mathcal{O}(m^{-6})$ -contribution to  $\gamma_{s, -}$  using (5.6) with  $I(m^2, 5) = \frac{2}{m^6}$  for (again log-spaced) caloron sizes between 0.001 and 100:

$$\begin{aligned} \frac{\gamma_{10}(\varrho)}{m^6} &= I(m^2, 5, 0; 0) \frac{1}{(4\pi)^2} \text{Tr}(\bar{b}_{10}) = \\ &= \begin{cases} -\frac{0.082}{\tilde{\varrho}^6 m^6} & : 0 < \varrho \leq 0.298 \\ -\frac{0.463}{\tilde{\varrho}^{3.87} m^6} + \frac{0.267}{\varrho^{5.33} m^6} & : 0.298 < \varrho \leq 1.348. \\ -\frac{2.280}{\varrho^{2.15} m^6} - \frac{5.106}{m^6} & : 1.348 < \varrho \end{cases} \end{aligned} \quad (5.12)$$

The fitting function has a relative error which is generally  $\leq 1\%$ . The small- $\varrho$  coefficient here is in good agreement with the instanton coefficient  $\frac{232}{2385}$  from [41]. We present our numerical results<sup>5</sup> in figure 8 and tabulate the numerical value in the ancillary materials.

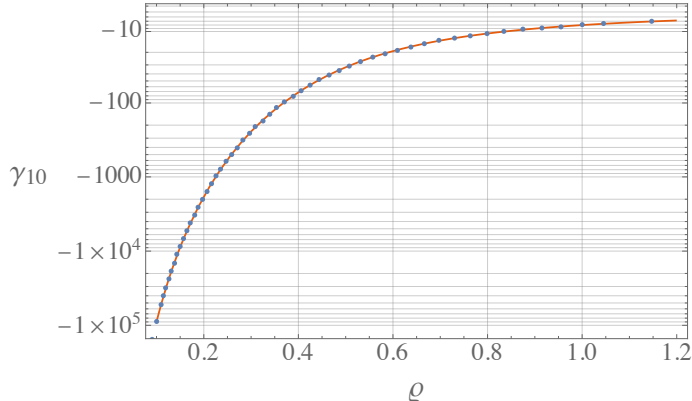


**Figure 8:**  $m^{-6}$ -coefficient  $\gamma_{10}$  (5.12) of  $\gamma_{s,-}$  (5.5).

**Order  $5 < k \in \mathbb{N}$ :**

Due to expected computational cost in calculating the explicit functional form of  $\bar{b}_{12}(x, \varrho)$  and numerical difficulties in performing  $\text{Tr}(\bar{b}_{12})$ , we do not obtain this contribution. For integer  $k > 6$  no heat kernel coefficients are known.

**Overall Result for  $m \gg 1$ :**

The regularized, vacuum - normalized Klein - Gordon operator determinant for a heavy, anti - periodic, complex scalar (5.5) then reads

$$\gamma_{s,-}(m \text{ large}, \varrho, \lambda) = \frac{1}{6} \ln\left(\frac{\lambda}{m}\right) - \frac{\gamma_6(\varrho)}{m^2} - \frac{\gamma_8(\varrho)}{m^4} - \frac{\gamma_{10}(\varrho)}{m^6}, \quad (5.13)$$

which is of the structure (3.3) with  $\gamma_{s,-}^{\text{large}, k} = \gamma_{2k}$  given by (5.10) - (5.12). Using this, we obtain the large - mass result for the fermionic correction factor (3.1):

$$\begin{aligned} f_{\text{ferm}}(m \geq m_{\text{large, min}}(\varrho), \varrho) &= f_{\text{large}}(m, \varrho) = \\ &= \frac{e^{-2\alpha(\frac{1}{2})}}{(m\varrho)^{\frac{1}{3}}} \exp\left(-\frac{2\gamma_6(\varrho)}{m^2} - \frac{2\gamma_8(\varrho)}{m^4} - \frac{2\gamma_{10}(\varrho)}{m^6}\right). \end{aligned} \quad (5.14)$$

In order to estimate the range of validity of (5.13) and (5.14), we demand that the successive terms become smaller in magnitude. For that, we find the “lightest heavy mass” so that 1)  $\frac{\gamma_6}{m^2} \geq \frac{\gamma_8}{m^4}$ , 2)  $\frac{\gamma_8}{\gamma_6 m^2} \geq \frac{|\gamma_{10}|}{\gamma_6 m^4 + \gamma_8 m^2}$ , and 3) the finite - temperature ambiguities discussed in appendix B are small compared to (5.13). From 1) and 2) we deduce the lower limit  $1.4\tilde{\varrho}^{-1}$  on  $m$  for  $\varrho \lesssim 1$  and  $m \gtrsim 2.8$  for larger  $\varrho$ . The lower mass limit  $m_{\text{large, min}, 3}(\varrho)$

<sup>5</sup>The authors would like to specifically thank Simon Stendebach for setting up the code for the numerical  $x$  - integration of  $\text{tr}(\bar{b}_{10})$  in (5.12) and performing the integrals (using the *Cubature* package [54–57] to handle the highly oscillatory integrand  $\text{tr}(\bar{b}_{10})$ ).

ensuring small  $T > 0$ -uncertainties is shown in [figure 15b](#) in [appendix B](#). All in all, the lower bound for the heavy quark mass expansion is

$$m_{\text{large, min}}(\varrho) = \max\left(\left\{\begin{array}{l} 1.4\tilde{\varrho}^{-1} : m \lesssim 1 \\ 2.8 : m \gtrsim 1 \end{array}\right\}, m_{\text{large, min, 3}}(\varrho)\right). \quad (5.15)$$

## 6 Interpolation and Application to the Susceptibility

Having performed the small- and large-mass expansions, we can use our results [\(4.18\)](#) and [\(5.14\)](#) for the fermionic part of the correction factor  $f_{\text{ferm}}$  [\(3.1\)](#) to perform the Padé approximation according to [\(3.5\)](#) - [\(3.7\)](#) as described in [section 3](#). Since we have an odd  $k_{\text{max}} = 3$  in [\(3.5\)](#), we set  $K = 1$  (cf. [\(3.7\)](#)) in [\(3.6\)](#).

$$\begin{aligned} -\ln(f_{\text{ferm}}(m, \varrho)) &= \gamma_{\text{ferm}} = 2\alpha\left(\frac{1}{2}\right) + p(m, \varrho) = \\ &= 2\alpha\left(\frac{1}{2}\right) + \begin{cases} -2\alpha\left(\frac{1}{2}\right) + \frac{(\pi\varrho)^2}{3} - 2A(\pi\varrho) - 2m^2\gamma_{\text{s, -}}^{\text{small}}(\varrho) & : m \leq m_{\text{small, max}}(\varrho) \\ \frac{1}{3}\ln(m\varrho) + \frac{2\gamma_6(\varrho)}{m^2} + \frac{2\gamma_8(\varrho)}{m^4} + \frac{2\gamma_{10}(\varrho)}{m^6} & : m \geq m_{\text{large, min}}(\varrho) \end{cases}. \end{aligned} \quad (6.1)$$

$${}^{k_{\text{max}}=3 \Rightarrow K=1} p(m, \varrho) = \frac{p_0(\varrho) + p_1(\varrho)m^2}{(1 + \mathcal{P}_1(\varrho)m^2)(1 + \mathcal{P}_2(\varrho)m^2)} + \frac{1}{6}\ln(m^2\varrho^2 + \xi^2(\varrho)). \quad (6.2)$$

Now we perform the Taylor and Laurent expansions of [\(6.2\)](#) for small and large masses up to  $\mathcal{O}(m^2)$  and  $\mathcal{O}(m^{-6})$ , respectively, and demand agreement with [\(6.1\)](#):

small- $m$  Taylor expansion:

$$p_0 + \frac{1}{6}\ln(\xi^2) + \left(p_1 - p_0\mathcal{P}_1 - p_0\mathcal{P}_2 + \frac{\varrho^2}{6\xi^2}\right)m^2 \stackrel{!}{=} -2\alpha\left(\frac{1}{2}\right) + \frac{(\pi\varrho)^2}{3} - 2A - 2m^2\gamma_{\text{s, -}}^{\text{small}}, \quad (6.3)$$

large- $m$  Laurent expansion:

$$\begin{aligned} \frac{1}{6}\ln(m^2\varrho^2) + \frac{6p_1\varrho^2 + \mathcal{P}_1\mathcal{P}_2\xi^2}{6\mathcal{P}_1\mathcal{P}_2m^2\varrho^2} + \frac{12p_0\mathcal{P}_1\mathcal{P}_2\varrho^4 - 12p_1\mathcal{P}_1\varrho^4 - 12p_1\mathcal{P}_2\varrho^4 - \mathcal{P}_1^2\mathcal{P}_2^2\xi^4}{12\mathcal{P}_1^2\mathcal{P}_2^2m^4\varrho^4} - \\ - \frac{18p_0\mathcal{P}_1^2\mathcal{P}_2\varrho^6 + 18p_0\mathcal{P}_1\mathcal{P}_2^2\varrho^6 - 18p_1\mathcal{P}_1^2\varrho^6 - 18p_1\mathcal{P}_1\mathcal{P}_2\varrho^6 - 18p_1\mathcal{P}_2^2\varrho^6 - \mathcal{P}_1^3\mathcal{P}_2^3\xi^6}{18\mathcal{P}_1^3\mathcal{P}_2^3m^6\varrho^6} \stackrel{!}{=} \\ \stackrel{!}{=} \frac{1}{6}\ln(m^2\varrho^2) + \frac{2\gamma_6}{m^2} + \frac{2\gamma_8}{m^4} + \frac{2\gamma_{10}}{m^6}. \end{aligned} \quad (6.4)$$

Using the  $m^2$ -,  $m^{-2}$ -,  $m^{-4}$ -, and  $m^{-6}$ -coefficient, we analytically solve for  $p_0(\varrho, \xi(\varrho))$ ,  $p_1(\varrho, \xi(\varrho))$ ,  $\mathcal{P}_1(\varrho, \xi(\varrho))$  and  $\mathcal{P}_2(\varrho, \xi(\varrho))$  and finally, using the  $\mathcal{O}(m^0)$ -terms, obtain  $\xi(\varrho)$

numerically. We find the following analytical results

$$p_0(\varrho, \xi(\varrho)) = \frac{\sqrt{2}}{12(-18\gamma_{10}\varrho^6 + \xi^6)} \left( \frac{3}{\sqrt{2}}(6\gamma_6\varrho^2 - \xi^2)(12\gamma_8\varrho^4 + \xi^4) + \frac{1}{\xi\varrho}\sqrt{q_1(\varrho, \xi)} \times \right. \\ \left. \times \sqrt{-6\gamma_{s,-}^{\text{small}}(\xi^8 - 18\gamma_{10}\xi^2\varrho^6) - 2\xi^6\varrho^2 + 18\gamma_6\xi^4\varrho^4 - 54\gamma_6^2\xi^2\varrho^6 + 9\gamma_{10}\varrho^8} \right), \quad (6.5)$$

$$p_1(\varrho, \xi(\varrho)) = \frac{6\gamma_6\varrho^2 - \xi^2}{3\left(\frac{q_5(\varrho, \xi)}{q_1} - \frac{\sqrt{3q_3(\varrho, \xi)}(12\gamma_8\varrho^4 + \xi^4)}{|q_1|}\right)} \left( \frac{q_2(\varrho, \xi)}{q_1} - \frac{\varrho^2\sqrt{3q_3}}{|q_1|} \right) \times \\ \times \left( \frac{q_4(\varrho, \xi)}{q_1} + \frac{\sqrt{3q_3}(6\gamma_6\varrho^2 - \xi^2)}{|q_1|} \right), \quad (6.6)$$

$$\mathcal{P}_1(\varrho, \xi(\varrho)) = \frac{q_2}{q_1} - \frac{\varrho^2\sqrt{3q_3}}{|q_1|}, \quad (6.7)$$

$$\mathcal{P}_2(\varrho, \xi(\varrho)) = \frac{2\varrho^2}{\frac{q_5}{q_1} - \frac{\sqrt{3q_3}(12\gamma_8\varrho^4 + \xi^4)}{|q_1|}} \left( \frac{q_4}{q_1} + \frac{\sqrt{3q_3}(6\gamma_6\varrho^2 - \xi^2)}{|q_1|} \right) \quad (6.8)$$

with

$$q_1(\varrho, \xi) = \xi^8 - 24\gamma_6\xi^6\varrho^2 - 72\gamma_8\xi^4\varrho^4 - 72\gamma_{10}\xi^2\varrho^6 - 432(\gamma_8^2 - \gamma_6\gamma_{10})\varrho^8, \quad (6.9)$$

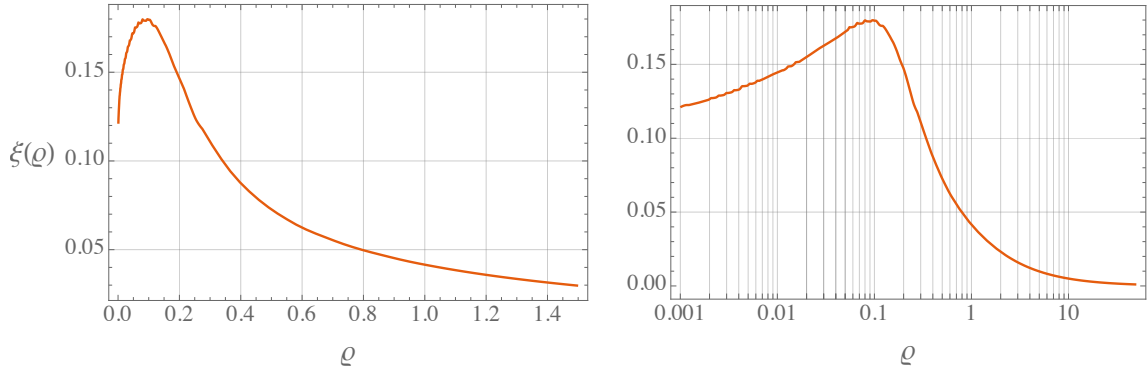
$$q_2(\varrho, \xi) = 3\left(- (1 + 4p_0^2)\xi^6\varrho^2 + \gamma_6\xi^4\varrho^4 - 12\gamma_8\xi^2\varrho^6 + 72(\gamma_6\gamma_8 + \gamma_{10}p_0)\varrho^8\right), \quad (6.10)$$

$$q_3(\varrho, \xi) = (7 + 36p_0 + 48p_0^2)\xi^{12} - 36\gamma_6(5 + 12p_0)\xi^{10}\varrho^2 + 108(13\gamma_6^2 - 2\gamma_8 - 4\gamma_8p_0)\xi^8\varrho^4 - \\ - 144\left(24\gamma_6^3 - 18\gamma_6\gamma_8(1 - 2p_0) + \gamma_{10}(2 + 9p_0 + 12p_0^2)\right)\xi^6\varrho^6 - \\ - 1296(6\gamma_6^2\gamma_8 - 2\gamma_6\gamma_{10}(2 + 3p_0) + \gamma_8^2(1 + 12p_0))\xi^4\varrho^8 + \\ + 15552(\gamma_6\gamma_8^2 - 2\gamma_6^2\gamma_{10} - \gamma_8\gamma_{10}p_0)\xi^2\varrho^{10} - \\ - 15552\left(3\gamma_6^2\gamma_8^2 - 4\gamma_6^3\gamma_{10} - 6\gamma_6\gamma_8\gamma_{10}p_0 + p_0(4\gamma_8^2 - \gamma_{10}^2p_0)\right)\varrho^{12}, \quad (6.11)$$

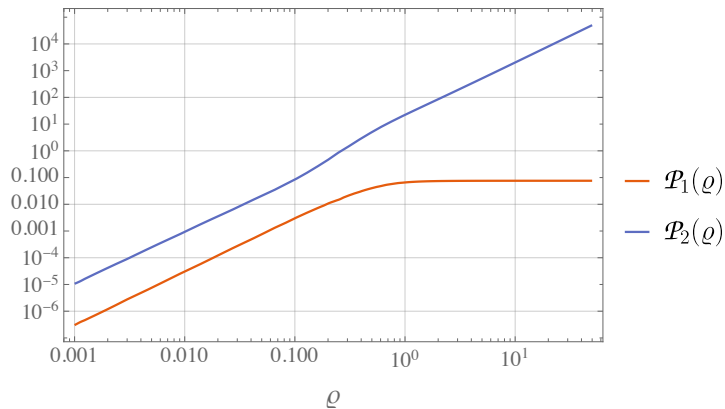
$$q_4(\varrho, \xi) = -3\left((1 + 2p_0)\xi^8 - 12\gamma_6(1 - 2p_0)\xi^6\varrho^2 + 12(3\gamma_6^2 + \gamma_8 + 12\gamma_8p_0)\xi^4\varrho^4 - \right. \\ \left. - 72(2\gamma_6\gamma_8 - \gamma_{10}p_0)\xi^2\varrho^6 + 432(\gamma_6^2\gamma_8 + 2\gamma_8^2p_0 - \gamma_6\gamma_{10}p_0)\varrho^8\right), \quad (6.12)$$

$$q_5(\varrho, \xi) = - (5 + 12p_0)\xi^{10} + 78\gamma_6\xi^8\varrho^2 - 72(4\gamma_6^2 - \gamma_8(1 - 2p_0))\xi^6\varrho^4 - \\ - 72(6\gamma_6\gamma_8 - \gamma_{10}(2 + 3p_0))\xi^4\varrho^6 + 432(\gamma_8^2 - 4\gamma_6\gamma_{10})\xi^2\varrho^8 - \\ - 2592(\gamma_6\gamma_8^2 - 2\gamma_6^2\gamma_{10} - \gamma_8\gamma_{10}p_0)\varrho^{10} \quad (6.13)$$

and the numerical results for  $\xi$  as shown in [figure 9a](#). In [figure 9b](#) we also show the parameters  $\mathcal{P}_1$  and  $\mathcal{P}_2$  and verify that they are indeed positive-definite functions as demanded in [\(3.6\)](#). Numerical values are tabulated in the ancillary files. Finally, in [figures 10](#) and [11](#) we present the full result of the ‘‘Padé-like’’ interpolation and the agreement with the small- and large-mass results given in [\(6.1\)](#).



(a) Numerical values for the parameter  $\xi(\varrho)$  of the “Padé-like” approximation (6.2), shown for the physically relevant caloron sizes  $\varrho$  (left) and for the full set of  $\varrho$ -values (right).



(b) The parameters  $\mathcal{P}_1(\varrho)$  and  $\mathcal{P}_2(\varrho)$  of (6.2), shown for the full set of  $\varrho$ -values; the parameters are positive-definite functions as demanded in (3.6).

**Figure 9**

Using the full fermionic correction factor  $f_{\text{ferm}}(m, \varrho)|_{T>0} = e^{-2\alpha(\frac{1}{2})-p(m, \varrho)}$  (6.1), we obtain the caloron density  $\mathcal{d}$  as given in (3.8) for the case of  $N = 3$ ,  $N_{f_l} = 4$  and  $N_{f_h} = 1$  (i.e., the heavy quark is the bottom quark). We show the caloron density, normalized by the maximum density of the asymptotic case  $m_b \rightarrow \infty$ , in figure 12. Our results shown in figure 12 also verify the small-constituent approximation, as introduced in the preliminaries, for finite  $T$  and with heavy quarks.

Lastly, we analyze the topological susceptibility  $\chi_{\text{top}}(m_{f_h}, T)$  and calculate the ratio  $\kappa$  (3.10), i.e., we compare two theories: one with physically heavy “non-light quarks” - which we analyzed in this work - and one where heavy quark masses are asymptotically large - which is accessible via lattice QCD. As we discussed in section 3, we modify the coupling constant for the asymptotic heavy mass-theory as given in (3.9), specifically, we match the theories to have the same IR behavior rather than to have the same UV value

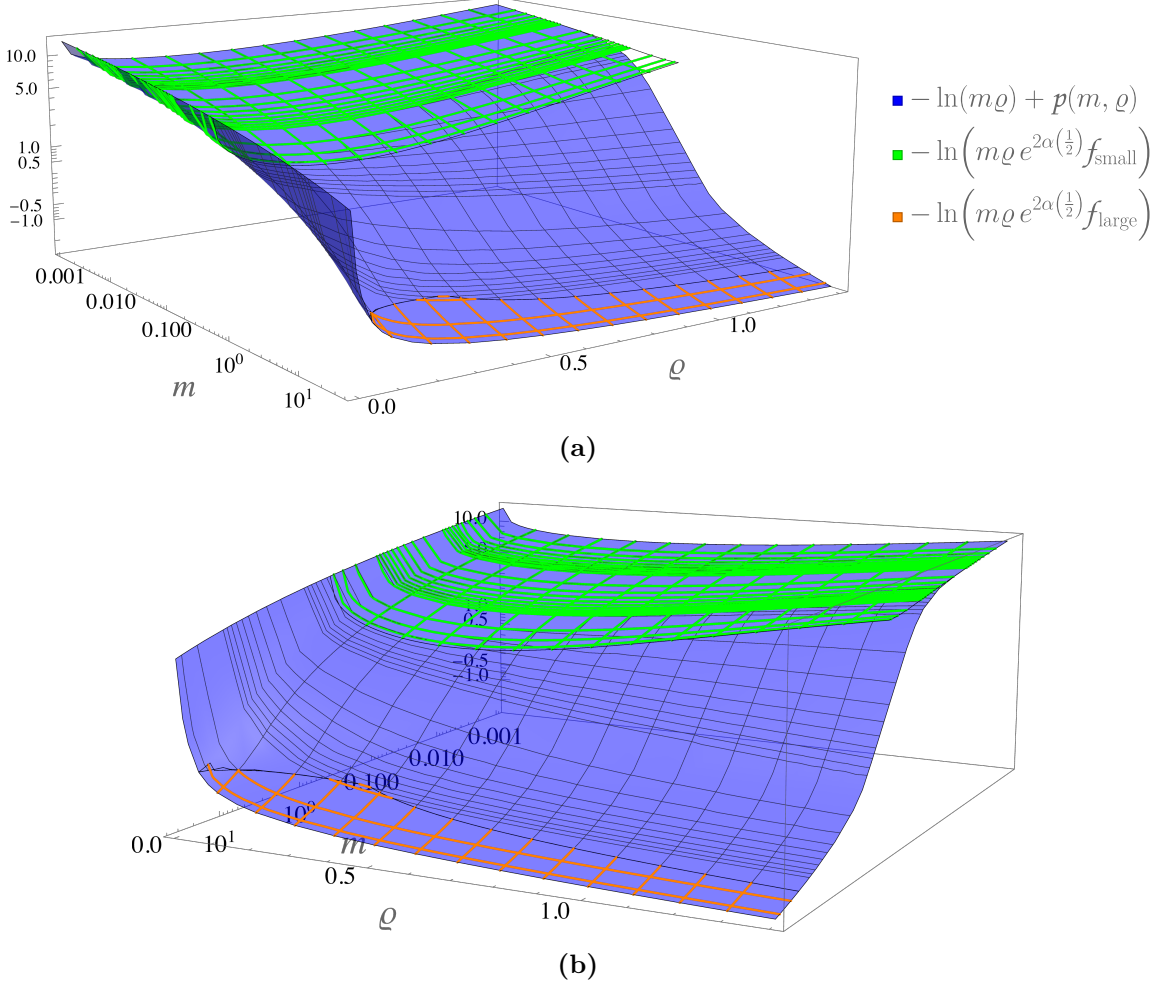


**Figure 10:** The negative logarithmic caloron density  $-\ln(\mathcal{d}) \supset -\ln(m\rho e^{2\alpha(\frac{1}{2})}f_{\text{ferm}})$  due to the heavy quark. **Green:** the small-mass expansion. **Orange:** the large-mass expansion. **Blue:** the “Padé-like” interpolation  $-\ln(m\rho) + p(m, \rho)$ , illustrating how well it matches to the two limiting behaviors in the regimes where they are expected to be accurate. The agreement with the small-mass expansion is poor at the largest  $\rho$  values, but otherwise the agreement is good wherever a small- or large-mass expansion is expected to work.

of the gauge coupling. In detail, the  $\chi_{\text{top}}$ -ratio reads

$$\kappa(m_{f_h}, N_{f_l}, N_{f_h}, N) = \frac{\int_0^\infty d\rho \rho^{\frac{11N+N_f}{3}-5} f(0, \rho)|_{N_{f_l}, N, T>0} \prod_{f_h} \sqrt[3]{m_{f_h}} e^{-p(m_{f_h}, \rho)}}{\int_0^\infty d\rho \rho^{\frac{11N+N_{f_l}}{3}-5} f(0, \rho)|_{N_{f_l}, N, T>0}}, \quad (6.14)$$

where the correction factor  $f(0, \rho)|_{N_{f_l}, N, T>0}$  for a full theory of only light quarks is given in (2.11).  $N_{f_l} = N_f - N_{f_h}$  in the denominator  $\rho$ -exponent is due to  $\lim_{m \rightarrow \infty} e^{-p} = (m\rho)^{-1/3}$ .

We calculate (6.14) for the physical case  $\kappa(m_b, 4, 1, 3)$  and  $b$  quark-masses between 0.011 and 25. As we discussed in section 1, this is our main result shown in figure 1.

We see that for (low) temperatures  $m_b \gtrsim \pi$  we find  $\kappa \gtrsim 0.95$ , i.e, the difference between the  $b$  quark and its infinitely heavy counterpart is less than 5%. Only for higher temperatures  $m_b \lesssim 2$  do we see  $\kappa \lesssim 0.9$  and a more than 10% difference between lattice QCD and physics with a dynamical  $b$  quark.

Our results indicate that, in the temperature range which is relevant for axion cosmology,  $T < 1100$  MeV, the effects of the heavy bottom quark on the topological susceptibility are below 10% when compared to working within the 4-quark theory with the same infrared coupling strength. For practical purposes this means that  $2+1+1$  mass simulations of QCD are sufficient for investigating the hot topological susceptibility for applications to axion cosmology.

## Acknowledgements

The authors acknowledge the support by the Deutsche Forschungsgemeinschaft (DFG, German Research Foundation) through the CRC-TR 211 ‘Strong-interaction matter under extreme conditions’ – project number 315477589 – TRR 211. The authors express particular thanks to Simon Stendebach for his help with numerical calculations in (5.12) and helpful discussions in general. The authors also thank Dietrich Bödeker and Rasmus Nielsen for useful conversations.

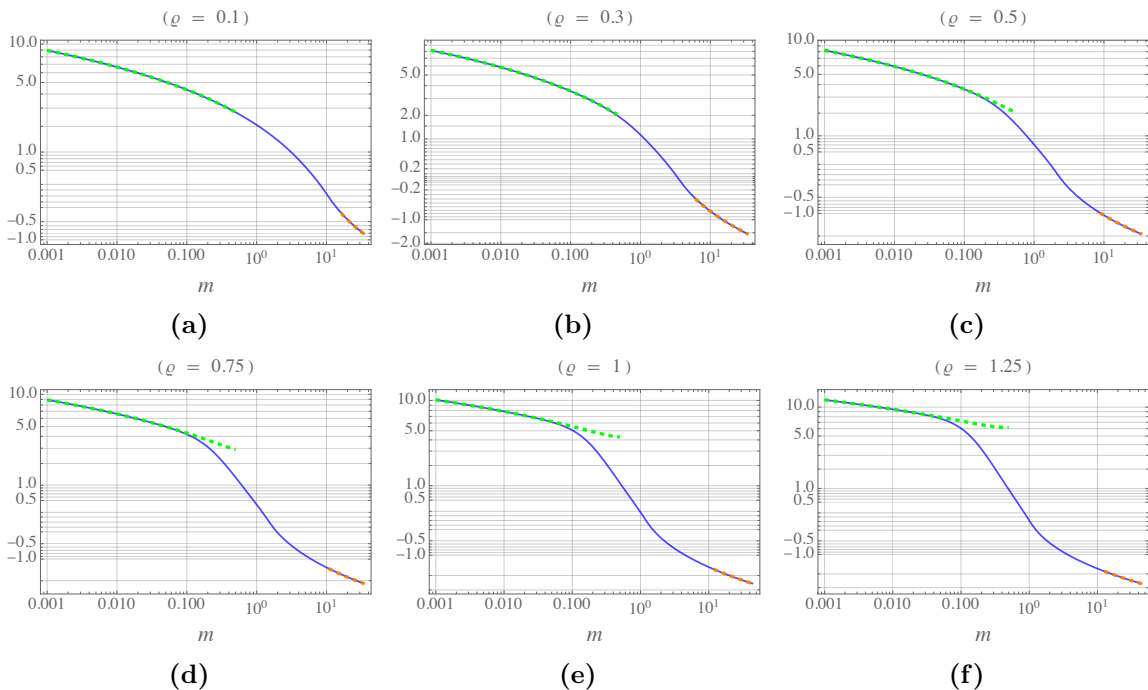


**Figure 11:** Finite-quark mass effect  $-\ln(m\rho e^{2\alpha(\frac{1}{2})}f_{\text{ferm}})$  as a function of  $m$  for several  $\rho$  values, corresponding to 2D slices from figure 10. The Padé approximation (—) shows good agreement with the large-mass result (— · —) and the small-mass result (---) within their expected ranges of validity, except that the small-mass expansion breaks down sooner than expected at the largest  $\rho$  values.

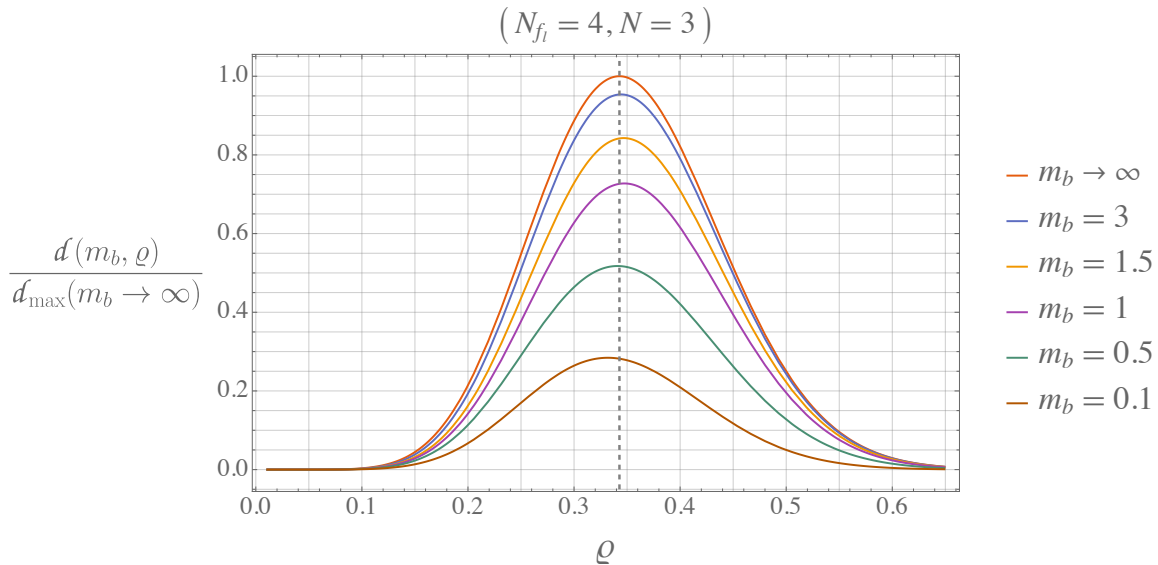


**Figure 12:** The caloron density  $d(N_{f_l}=4, N=3, m_b, \varrho, \lambda)$  (3.8) with the correction factor  $e^{-2\alpha(\frac{1}{2})-p(m, \varrho)}$  (6.1). We normalize it by the maximum density of the 4-flavor theory, represented by  $d_{\max}(m_b \rightarrow \infty, g_{\text{asy}})$  with  $g_{\text{asy}}$  as in (3.9), which is located at  $\varrho \approx 0.343$  (vertical dashed line). Decreasing mass decreases the caloron density and slightly shifts the location of the peak, to larger  $\varrho$  at large mass  $m > 1$  and to smaller  $\varrho$  at small mass  $m < 0.5$ .

## A Partial Differential Equation

In order to solve the full problem of the topological susceptibility’s quark mass dependence at finite temperatures, one has to compute the determinant ratio  $\frac{\det(-D_-^2 + m_f^2) \det(-\partial_-^2 + \lambda^2)}{\det(-D_-^2 + \lambda^2) \det(-\partial_-^2 + m_f^2)}$  (cf. (2.7)), i.e., one has to solve the eigenvalue problem

$$(-D_-^2 + m^2)\psi_n = \lambda_n \psi_n. \quad (\text{A.1})$$

given in terms of coupled ordinary and partial differential equations (ODEs and PDEs). We derive these differential equations in the following.

Following [5], the spacetime  $\mathbb{R}^3 \times S_{\text{rad}=1/2\pi}^1$  can be separated into three regions as depicted in figure 13: the “instanton region” I with  $|(\vec{x}, \tau)| = \sqrt{r^2 + \tau^2} \ll 1$ , the “asymptotic region” III with  $r = \sqrt{\vec{x}^2} \gg 1$  and the “transition region” II in between.

In the instanton region I the caloron  $A_{\text{HS}}^{a\mu} = -\bar{\eta}^{a\mu\nu} \partial^\nu \ln(\phi)$  (2.1) resembles an instanton of modified size  $\tilde{\varrho}$  (cf. (2.4) and (2.5)) [5]. The behavior of individual solutions to (A.1) in this region are the same as for an instanton. This determines the small-radius boundary conditions for the solutions in the transition region.

In the asymptotic region III we can expand  $\phi \xrightarrow{r \gg 1} 1 + \frac{\pi \varrho^2}{r} + \pi^2 \varrho^2 \mathcal{O}(re^{-\pi r})$ . This obeys 3-dimensional radial symmetry and the resulting asymptotic caloron components read  $A_{\text{HS}}^{a4} \xrightarrow{r \gg 1} \frac{1-r}{1+\frac{r}{\pi \varrho^2}} \frac{x^a}{r^2} = a_\varrho^{\text{III}}(r) \frac{x^a}{r^2}$  and  $A_{\text{HS}}^{ai} \xrightarrow{r \gg 1} a_\varrho^{\text{III}}(r) \varepsilon^{aij} \frac{x^j}{r^2}$ , i.e., the caloron is static in  $\tau$ . We can thus exploit this radial symmetry by adapting the approach developed in



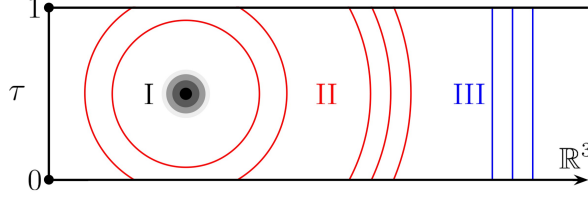


**Figure 13:** The three spacetime regions important for solving (A.1). As in figure 5, the caloron is shown as a graded gray sphere. In the “instanton region” I the caloron resembles a 4-dimensional radially symmetric instanton; in the “asymptotic region” III the caloron is reduced to a 3-dimensional, radially symmetric object. The topology of  $\mathbb{R}^3 \times S^1_{\text{rad}=1/2\pi}$  with its distinct, bounded time direction and open space directions and the resulting broken down symmetry group (cf. the discussion at the end of the preliminaries) are relevant in the asymptotic region III as well as the “transition region” II.

[30]: we use the regular angular momentum operators  $L^a = -i \varepsilon^{aij} x^i \partial^j$  and define the isospin operators  $\mathcal{T}^a = \frac{\sigma^a}{2}$  as well as the “spin + isospin” operators  $J^a = L^a + \mathcal{T}^a$ . This means that  $L^2$  has eigenvalues  $l(l+1)$ ,  $l \in \mathbb{N} \cup \mathbb{N} + \frac{1}{2}$ ,  $\mathcal{T}^2$  has the eigenvalue  $\frac{3}{4}$  and  $J^2$  has eigenvalues  $j(j+1)$ ,  $j = |l \pm \frac{1}{2}|$ . Using this, we find the  $-D_-^2$ -operator in region III:

$$\begin{aligned} -D_-^2 &= -\partial_r^2 - \frac{2}{r} \partial_r + \frac{L^2}{r^2} + 2a_\varrho^{\text{III}}(r) \frac{\vec{L} \cdot \vec{\mathcal{T}}}{r^2} + \frac{(a_\varrho^{\text{III}}(r))^2}{r^2} \mathcal{T}^2 - \partial_\tau^2 + \frac{2ia_\varrho^{\text{II}}(r)}{r} \hat{e}_r \cdot \vec{\mathcal{T}} \partial_\tau = \\ &= -\partial_r^2 - \frac{2}{r} \partial_r + \frac{l(l+1)}{r^2} + a_\varrho^{\text{III}} \frac{(j-l)(j+l+1)}{r^2} - \frac{3(a_\varrho^{\text{III}})^2}{4r\pi\varrho^2} - \partial_\tau^2 + \frac{2ia_\varrho^{\text{III}}}{r} \hat{e}_r \cdot \vec{\mathcal{T}} \partial_\tau, \end{aligned} \quad (\text{A.2})$$

where we used a separation Ansatz for the eigenfunction  $\psi_{n,l,j}(x) = \chi_{l,j}(\theta, \varphi) \tilde{\Psi}_{n,l,j}(r, \tau)$  with  $\chi_{l,j}$  a function and  $\tilde{\Psi}_{n,l,j}$  a 2-spinor. Furthermore, in the asymptotic limit  $r \gg 1$  with  $\tau$ -independent calorons any  $\psi_n$  can be expanded in terms of fermionic Matsubara frequencies  $p_\alpha^f \in \mathbb{Z} = 2\pi(\alpha + \frac{1}{2})$ , i.e.,  $\psi_{n,l,j}(x) = \chi_{l,j}(\theta, \varphi) \sum_{\alpha \in \mathbb{Z}} \tilde{\Psi}_{n,l,j,\alpha}(r, p_\alpha^f) e^{-ip_\alpha^f \tau}$ . This gives us the  $-D_-^2$ -operator as it acts on  $\tilde{\Psi}_{n,l,j,\alpha}$ :

$$-D_-^2 = -\partial_r^2 - \frac{2}{r} \partial_r + \frac{l(l+1)}{r^2} + a_\varrho^{\text{III}} \frac{(j-l)(j+l+1)}{r^2} + \frac{3(a_\varrho^{\text{III}})^2}{4r\pi\varrho^2} - (p_\alpha^f)^2 + \frac{2a_\varrho^{\text{III}} p_\alpha^f}{r} \hat{e}_r \cdot \vec{\mathcal{T}}. \quad (\text{A.3})$$

Note that (A.3) gives a coupled system of two ODEs due to the isospin operators  $\mathcal{T}^a$  (alternatively:  $\hat{e}_r \cdot \vec{\mathcal{T}} = \frac{\sigma^r}{2}$ ). Together with (A.1) this is the eigenvalue problem in the asymptotic region which gives the boundary conditions for the transition region solutions.

For the transition region II we again introduce  $L^a$  and  $\mathcal{T}^a$  together with the separation Ansatz  $\psi_{n,l,j}(x) = \chi_{l,j}(\theta, \varphi) \Psi_{n,l,j}(r, \tau)$ . Additionally, we define the function  $\Phi = \frac{\phi(r,\tau)}{r}$ , so that  $A_{\text{HS}}^a = -(1 + r \frac{\partial_r \Phi}{\Phi}) \frac{x^a}{r^2} = -a_\varrho^{\text{II}}(r, \tau) \frac{x^a}{r^2}$  and  $A_{\text{HS}}^{ai} = -a_\varrho^{\text{II}}(r, \tau) \varepsilon^{aij} \frac{x^j}{r^2} + \delta^{ai} \frac{\partial_r \Phi}{\Phi}$ . We thus find the differential operator acting on  $\Psi_{n,l,j}$ :

$$\begin{aligned} -D_-^2 &= -\partial_r^2 - \frac{2}{r} \partial_r + \frac{L^2}{r^2} + 2a_\varrho^{\text{II}}(r, \tau) \frac{\vec{L} \cdot \vec{\mathcal{T}}}{r^2} + i \partial_r \frac{\partial_r \Phi}{\Phi} \hat{e}_r \cdot \vec{\mathcal{T}} - i \partial_\tau \frac{\partial_r \Phi}{\Phi} + \\ &+ \frac{(a_\varrho^{\text{II}}(r, \tau))^2}{r^2} \mathcal{T}^2 + \left( \frac{\partial_r \Phi}{\Phi} \right)^2 \mathcal{T}^2 - \partial_\tau^2 - \frac{2ia_\varrho^{\text{II}}(r, \tau)}{r^2} \hat{e}_r \cdot \vec{\mathcal{T}} \partial_\tau = \end{aligned}$$

$$\begin{aligned}
&= -\partial_r^2 - \frac{2}{r}\partial_r + \frac{l(l+1)}{r^2} + a_\rho^{\text{II}} \frac{(j-l)(j+l+1)}{r^2} + i\partial_r \frac{\partial_\tau \Phi}{\Phi} \hat{e}_r \cdot \vec{\mathcal{T}} - \\
&\quad - i\partial_\tau \frac{\partial_r \Phi}{\Phi} + \frac{3}{4} \frac{a_\rho^{\text{II}}}{r} \frac{\partial_r \Phi}{\Phi} + \frac{3}{4} \left( \frac{\partial_\tau \Phi}{\Phi} \right)^2 - \partial_\tau^2 - \frac{2ia_\rho^{\text{II}}}{r^2} \hat{e}_r \cdot \vec{\mathcal{T}} \partial_\tau.
\end{aligned} \tag{A.4}$$

Since  $\Psi_{n,l,j}$  cannot be expanded in terms of Matsubara frequencies in this region, the transition region-eigenvalue problem given by (A.4) and (A.1) is posed in terms of a two-dimensional, coupled system of PDEs.<sup>6</sup> These are to be matched at small and large  $\sqrt{r^2 + \tau^2}$  to the asymptotic forms in the other two regions.

## B Boundary Condition – Dependence at large Mass

Our calculation of the large-mass expansion in section 5.1 leads to results which do not depend on the boundary conditions (periodic or anti-periodic) of the differential operator  $D_\pm^2$ . Clearly the full finite-mass results do depend on these boundary conditions, and therefore the asymptotic large-mass expansion must be an asymptotic series with exponentially suppressed trans-series corrections of form  $m^b e^{-m}$  which do depend on the boundary conditions and which represent an ambiguity in the resummation of the large-mass expansion. Our goal in this appendix is to determine this behavior, which gives the difference between symmetric and anti-symmetric boundary conditions. This difference gives us information on the limitations of the order-by-order large-mass expansion, which helps us understand the range of reliability of said expansion.

The periodicity-dependent coefficients depend not only on the chromo-electric and chromo-magnetic fields  $E^i = G^{i4}$  and  $B^i = \frac{1}{2}\epsilon^{ijk}G^{jk}$  and their covariant derivatives, but also on dimensionless, matrix-valued coefficient functions

$$\varphi_l(\vec{x}, \rho, s) = \sum_{\alpha \in \mathbb{Z}} \sqrt{4\pi s} \frac{l+1}{2} \left( ip_\alpha^{\text{b/f}} - \ln \Omega(\vec{x}, \rho) \right)^l e^{s(ip_\alpha^{\text{b/f}} - \ln \Omega(\vec{x}, \rho))}, \tag{B.1}$$

where  $p_\alpha^{\text{b/f}}$  are again the bosonic/fermionic Matsubara frequencies (we use the  $p_\alpha^{\text{f}}$ ) and

$$\Omega(\vec{x}, \rho) = \text{T exp} \left( i \int_0^1 d\tau A_{\text{HS}}^4(\vec{x}, \tau) \right) = \exp(i\pi \omega(r, \rho) \sigma^r) \in SU(2) \tag{B.2}$$

is the Polyakov loop<sup>7</sup> with  $A_{\text{HS}}^4 = -\frac{\partial_\tau \phi}{\phi} \frac{\sigma^r}{2}$  (note that  $[\Omega] = [\varphi_l] = 1$ ). The known coeffi-

<sup>6</sup>If one aims to solve this eigenvalue problem, one could expand  $\Phi(r, \tau)$  in terms of radial and temporal variables  $u, v$  given by  $r = 1 + u$  and  $\tau = 1 - v$ , respectively. This simplifies the coefficient functions in (A.4) to rational functions of  $u$  and  $v$ , thus possibly simplifying calculations, reducing numerical cost and/or making possible the application of certain theorems from the theory of partial differential equations.

<sup>7</sup>The function  $-\pi\omega(r, \rho)$  is given in [58, eq. (59)].

icients  $b_{2k}$  for the heat kernel  $\langle x|e^{-(D_-^2)s}|x\rangle$  read:

$$\begin{aligned}
b_0(A_{\text{HS}}) &= \varphi_0, & b_{\text{free}} &= b_0(0) = \varphi_0(\varrho = 0), & b_4(A_{\text{HS}}) &= \varphi_0 \bar{b}_4 - \frac{\varphi_0 + 2\varphi_2}{6} \vec{E}^2, \\
b_6(A_{\text{HS}}) &= \varphi_0 \bar{b}_6 + \frac{\varphi_0 + 2\varphi_2}{60} \left( (\vec{D} \cdot \vec{E})^2 + 2(D_\tau \vec{B})^2 + \vec{E} \cdot (\vec{B} \times \vec{E}) \right) - \\
&\quad - \left( \frac{\varphi_0}{15} + \frac{\varphi_2}{3} + \frac{2\varphi_4}{15} \right) (D_\tau \vec{E})^2, \\
b_{8 \leq 2k \leq 12}(A_{\text{HS}}) &= \varphi_0 \bar{b}_{2k} + \text{“unknown”};
\end{aligned} \tag{B.3}$$

the other coefficients either vanish in general ( $2k \in \{1, 3\}$ ) or for  $-D_-^2$  ( $2k \in \{2, 5\}$ ), are unknown beyond  $\varphi_0 \bar{b}_{2k}$  ( $6 < 2k \leq 12$  and  $2k = \text{even}$ ) or are completely undetermined ( $2k > 6$  and  $2k = \text{odd}$ ).

In [49, 50] it is shown how  $\varphi_0$  can be transformed using Poisson’s summation formula for Fourier series: treating  $\tilde{f}(p) = \exp((ip - \ln \Omega)^2)$  as a continuous, aperiodic function of  $p \in \mathbb{R}$  with a Fourier transform  $f(\tau)$ , one has  $\sum_{p \in \mathbb{Z}} \tilde{f}(p) = \sum_{j \in \mathbb{Z}} f(j)$ . This yields

$$\varphi_0 = \sum_{\alpha \in \mathbb{Z}} \sqrt{4\pi s} e^{s(ip_\alpha^{b/f} - \ln(\Omega))^2} = \sum_{j \in \mathbb{Z}} (\pm 1)^j \Omega^j e^{-\frac{j^2}{4s}} \tag{B.4}$$

with  $\pm 1$  for the bosonic/fermionic case and  $\Omega^j(\vec{x}, \varrho) = \cos(j\pi \omega(r, \varrho)) + i \sin(j\pi \omega(r, \varrho)) \sigma^r$ . This Fourier back - transformation, which is easier evaluated, connects the momentum space of Matsubara frequencies back to proper time  $s$ . The heat kernel  $\langle x|e^{-(D_-^2)s}|x\rangle$ , as a proper time - propagator, then yields a closed loop propagator in Euclidean time  $\Delta^-(x, x, m^2)$  (cf. (4.3)) via  $s$ -integration (5.2). Here, the  $j = 0$ -mode corresponds to aperiodic loops in the heat kernel expansion - cf. figure 3 -, while  $j \neq 0$ -modes correspond to anti-periodically closed loops and thus constitute the finite- $T$  ambiguities.

All finite- $T$  terms with  $j \neq 0$  are exponentially suppressed in  $s$  compared to the leading contribution  $j = 0$ , but appear in the infinite  $j$ -summations. We compute them and show that these ambiguities are also suppressed compared to the large- $m$  expansion (5.13). In (B.5) we show that only  $\varphi_0$  in (B.3) contains  $j = 0$ -terms, i.e., only the  $\bar{b}_{2k}$  contribute to the heat kernel expansion which we used in section 5.2. Everything else, i.e., the  $j \neq 0$ -modes of  $\varphi_0$  and the  $\varphi_l$ -combinations, constitute the aforementioned finite-temperature uncertainties.

We use the Poisson summation formula - trick that gave (B.4) to calculate higher  $\varphi_{l>0}$ . For that, we write  $\varphi_l(a) = \sum_p \sqrt{4\pi} s^{(l+1)/2} Q^l e^{sQ^2 + aQ}$  with  $Q = ip - \ln(\Omega)$  and obtain the general form  $\varphi_l = s^{l/2} (\partial_a^{(l)} \varphi_0(a))|_{a=0}$ . Now we Fourier transform  $\varphi_0(a)$ , employ the Poisson formula and perform the  $a$ -derivatives before finally setting  $a = 0$ . For the  $\varphi_l$ -combinations appearing in (B.3) we find:

$$\varphi_0 + 2\varphi_2 = \sum_{j \in \mathbb{Z}} (\pm 1)^j \Omega^j e^{-\frac{j^2}{4s}} \frac{j^2}{2s}, \quad \frac{\varphi_0}{15} + \frac{\varphi_2}{3} + \frac{2\varphi_4}{15} = \sum_{j \in \mathbb{Z}} (\pm 1)^j \Omega^j e^{-\frac{j^2}{4s}} \frac{j^2(j^2 - 2s)}{120s^2}. \tag{B.5}$$

All modes  $j \neq 0$  are exponentially suppressed and for both combinations in (B.5) the  $j = 0$ -mode vanishes identically. The limit  $s \rightarrow 0$  reproduces the  $j = 0$ -modes and we

thus see that the known finite- $T$  terms in (B.3) vanish exponentially for  $T \rightarrow 0 \Rightarrow s \rightarrow 0$ , just as expected.

In order to calculate the boundary condition-dependent finite- $T$  uncertainties, we need to modify the  $s$ -integrals (5.6) to include the  $j \neq 0$ -modes. In general, we consider

$$\begin{aligned} I(m^2, k, j^2; c) &= \int_0^\infty ds e^{-m^2 s - \frac{j^2}{4s}} s^{k-3-c} = 2^{-(k-3-c)} \left(\frac{|j|}{m}\right)^{k-2-c} K_{|k-2-c|}(|j|m) m^2 \gg 1 \\ &\sim 2^{-(k-\frac{5}{2}-c)} \sqrt{\pi} \frac{|j|^{k-\frac{5}{2}-c}}{m^{k-\frac{3}{2}-c}} e^{-|j|m} \left(1 + \sum_{u \in \mathbb{N}^+} \frac{\prod_{v=1}^u (4(k-2-c)^2 - (2v-1)^2)}{u!(8|j|m)^u}\right) \end{aligned} \quad (\text{B.6})$$

with  $c \in \mathbb{N}$  resulting from the  $\varphi_l$ -combinations (B.5) and  $K_\alpha(x)$  the modified Bessel function of the second kind. Note that for the  $j$ -summation  $I(m^2, k, j^2; c)$  has to be multiplied by the corresponding factor  $\propto j^{2c}$  from the terms (B.5). Since the  $K_\alpha$ -expansion is an asymptotic one, it is justified for large (enough)  $|j|m$  to keep only the first few terms. These integrals (B.6) are  $e^{-m}$ -damped, but part of the infinite  $j$ -summation. Therefore, we compute the total finite- $T$  terms to quantify the large enough masses required to keep these terms suppressed compared to (5.13).

**Order  $k = 0$ :**

For the  $j \neq 0$ -modes of  $b_0(A_{\text{HS}})$  and  $b_{\text{free}}$  we find finite  $s$ -integrals  $I(m^2, 0, j^2; 0)$ . Performing the  $j$ -summation of  $\varphi_0$  (B.4), we obtain

$$\sum_{j \in \mathbb{Z} \setminus \{0\}} (-1)^j \Omega^j 2^{\frac{5}{2}} \sqrt{\pi} \frac{m^{\frac{3}{2}}}{|j|^{\frac{5}{2}}} e^{-|j|m} \left(1 + \frac{15}{8|j|m} + \mathcal{O}(m^{-2})\right). \quad (\text{B.7})$$

Here we neglect all contributions which are mass damped by inverse powers of  $m$  with respect to the  $j = 0$ -mode: for  $k = 0$  the ‘‘leading’’ term is 0 and thus  $\mathcal{O}(m^0)$ . Therefore, we neglect all terms  $\mathcal{O}(m^{-1/2})$  and lower in (B.7). We plug in  $\Omega^j$  and keep only the traceful part  $\cos(j\pi\omega)$ :

$$\begin{aligned} &\sum_{j \in \mathbb{Z} \setminus \{0\}} (-1)^j \Omega^j 2^{\frac{5}{2}} \sqrt{\pi} \frac{m^{\frac{3}{2}}}{|j|^{\frac{5}{2}}} e^{-|j|m} \left(1 + \frac{15}{8|j|m}\right) =_{\text{tr}} \\ &=_{\text{tr}} \sum_{j \in \mathbb{N}^+} (-1)^j \cos(j\pi\omega) 2^{\frac{7}{2}} \sqrt{\pi} \frac{m^{\frac{3}{2}}}{j^{\frac{5}{2}}} e^{-jm} \left(1 + \frac{15}{8jm}\right) = \\ &= 2^{\frac{7}{2}} \sqrt{\pi} \left(m^{\frac{3}{2}} \text{Re}(\text{Li}_{\frac{5}{2}}(-e^{i\pi\omega-m})) + \frac{15}{8} m^{\frac{1}{2}} \text{Re}(\text{Li}_{\frac{7}{2}}(-e^{i\pi\omega-m}))\right) = \\ &= 2^{\frac{7}{2}} \sqrt{\pi} \left(\text{L}_{\frac{3}{2}, \frac{5}{2}}(m, \omega(r, \varrho)) + \frac{15}{8} \text{L}_{\frac{1}{2}, \frac{7}{2}}(m, \omega(r, \varrho))\right), \end{aligned} \quad (\text{B.8})$$

where  $\text{Li}_b(z)$  is the polylogarithm and we introduced the function

$$\text{L}_{a,b}(m, \omega(r, \varrho)) = m^a \text{Re}(\text{Li}_b(-e^{i\pi\omega(r, \varrho)-m})). \quad (\text{B.9})$$

For general heat kernel contributions  $\mathcal{O}(m^d)$  our rule about dropping mass damped terms thus translates to neglecting all contributions  $L_{a,b}$  with  $a < d$ .<sup>8</sup> The free case is calculated analogously with  $\Omega = 1 \Leftrightarrow \omega = 0$  and we have

$$2^{\frac{7}{2}}\sqrt{\pi}\left(m^{\frac{3}{2}}\text{Li}_{\frac{5}{2}}(-e^{-m}) + \frac{15m^{\frac{1}{2}}}{8}\text{Li}_{\frac{7}{2}}(-e^{-m})\right). \quad (\text{B.10})$$

The overall finite- $T$  term at  $k = 0$  is thus given by<sup>9</sup>

$$\begin{aligned} \gamma_0^T(m, \varrho) = & \frac{2^{\frac{5}{2}}}{\sqrt{\pi}} \int_0^\infty dr r^2 \left( L_{\frac{3}{2}, \frac{5}{2}}(m, \omega(r, \varrho)) + \frac{15}{8} L_{\frac{1}{2}, \frac{7}{2}}(m, \omega(r, \varrho)) - \right. \\ & \left. - m^{\frac{3}{2}} \text{Li}_{\frac{5}{2}}(-e^{-m}) - \frac{15m^{\frac{1}{2}}}{8} \text{Li}_{\frac{7}{2}}(-e^{-m}) \right). \end{aligned} \quad (\text{B.11})$$

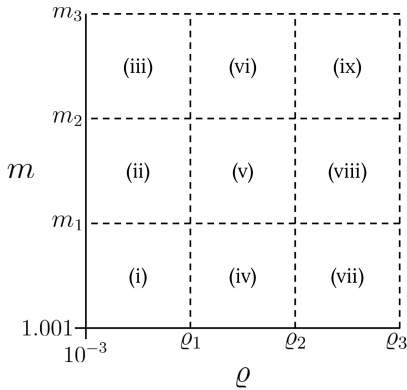


**Figure 14**

We compute  $\gamma_0^T$  on a grid in the  $m$ - $\varrho$ -plane, which we split in nine sectors (i) - (ix) as shown in [figure 14](#).

It is difficult to provide a good functional fit to the  $\gamma_0^T$ -data, which we obtained using the *SymPy* [59] and *mpmath* [60] packages<sup>10</sup> (this is indeed the case for all finite-temperature terms); the best approximation is given by the function

$$\zeta(m, \tilde{\varrho}; \tilde{a}, \tilde{b}, \tilde{c}, a, b, c) = e^{-m} \left( \tilde{a} m^{\tilde{b}} \tilde{\varrho}^{\tilde{c}} + a m^b \varrho^c \right), \quad (\text{B.12})$$

which serves to provide an intuition for the general functional form.

The coefficients  $\tilde{a}$ ,  $\tilde{b}$ ,  $\tilde{c}$ ,  $a$ ,  $b$ ,  $c$  for  $\gamma_0^T$  and the sector boundaries are given in [table 1](#). The boundaries given in [table 1](#) are roughly set by hand to minimize the fitting error: the fit agrees with our numerical data to within about 5%. As a consequence of (B.12),  $\gamma_0^T(\lambda, \varrho)$  vanishes exponentially as  $\lambda \rightarrow \infty$  (and analogously for  $k > 0$ ).

Our  $\gamma_0^T$ -data and the corresponding fitting error-data as well as the data for  $k = 2$  and  $k = 3$  (see below) can be found in the ancillary files. We showed that despite the infinite  $j$ -summation, the finite- $T$  uncertainties reflecting the boundary conditions are exponentially small as  $m^b e^{-m}$ ,  $b \sim 1$  for large enough masses.

<sup>8</sup>The pattern of  $a$  decreasing and  $b$  increasing in units steps in  $L_{a,b}$  as shown in (B.8) is universal to the finite- $T$  terms due to (B.6).

<sup>9</sup>Including an additional factor of  $(2\pi)^{-1}$  due to a factor of 2 from  $\text{tr}(1 \in \mathfrak{su}(2))$ , the heat kernel expansion prefactor  $(4\pi)^{-2}$  and the volume element  $4\pi r^2 dr$ ; the integral  $\int_0^1 d\tau$  is trivial and yields 1.

<sup>10</sup>These packages allows us to handle polylogarithms in symbolic and numerical *Python*-calculations, respectively.

	(i)	(ii)	(iii)	(iv)	(v)	(vi)	(vii)	(viii)	(ix)
$\tilde{a}$	8.878	8.107	5.000	$\tilde{a}_0^{(1)}(\varrho)$	$\tilde{a}_0^{(2)}(\varrho)$	$\tilde{a}_0^{(3)}(\varrho)$	0	0	0
$\tilde{b}$	1.03	1.17	1.42	1.03	1.17	1.42	0	0	0
$\tilde{c}$	3.00	3.00	3.00	3.13	3.13	3.13	0	0	0
$a$	0	0	0	$a_0^{(1)}(\varrho)$	$a_0^{(2)}(\varrho)$	$a_0^{(3)}(\varrho)$	3.075	2.823	1.700
$b$	0	0	0	1.04	1.18	1.42	1.04	1.18	1.43
$c$	0	0	0	2.25	2.26	2.26	2.00	2.00	2.00

**Table 1:** The sector boundaries for  $\gamma_0^T$  are  $m_1 \approx 2$ ,  $m_2 \approx 8$ ,  $\varrho_1 \approx 0.22$ ,  $\varrho_2 \approx 1.2$ ;  $m_3 = \varrho_3 = 200$ . The functions  $\tilde{a}(\varrho)$  and  $a(\varrho)$  in sectors (iv) - (vi) are required due to the rapid transition from small caloron ( $\tilde{\varrho}$ ) to large caloron description ( $\varrho$ ). They contain step functions  $\Theta_l(\varrho, u) = (1 + e^{-2u\varrho})^{-1}$ :  $\tilde{a}_0^{(1)} = 11.24(1 - \Theta_l(\varrho - 0.4, 7.5))$ ,  $\tilde{a}_0^{(2)} = 10.29(1 - \Theta_l)$ ,  $\tilde{a}_0^{(3)} = 6.350(1 - \Theta_l)$ ,  $a_0^{(1)} = 2.904\Theta_l$ ,  $a_0^{(2)} = 2.657\Theta_l$ ,  $\tilde{a}_0^{(3)} = 1.650\Theta_l$ .

**Order  $k > 0$ :**

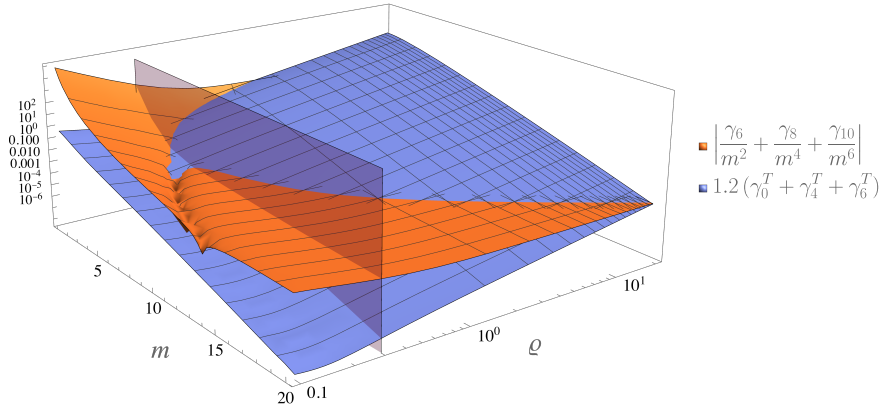
For  $k = 2$  we have  $j \neq 0$ -terms  $\propto (\mathbb{L}_{-\frac{1}{2}, \frac{1}{2}} + \dots)\bar{b}_4$  from  $\varphi_0$ , which we neglect as mass damped, and the following boundary condition term from  $\frac{1}{6}(\varphi_0 + 2\varphi_2)$ :

$$\gamma_4^T(m, \varrho) = -\frac{1}{2^{\frac{5}{2}} \cdot 3\sqrt{\pi}} \int_0^1 d\tau \int_0^\infty dr r^2 \mathbb{L}_{\frac{1}{2}, -\frac{1}{2}}(m, \omega(r, \varrho))(E^{ai}E^{ai})(r, \tau, \varrho). \quad (\text{B.13})$$

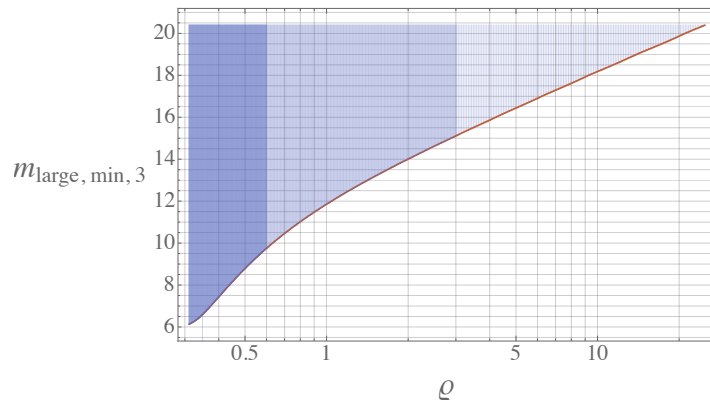
At heat kernel order  $k = 3$  the finite-temperature terms read (one has to be careful about the  $\mathfrak{su}(2)$ -traces; note that, e.g.,  $E^{ai;i} = (\vec{D} \cdot \vec{E})^a$  and  $E^{ai;4} = (D_\tau E^i)^a$ )

$$\begin{aligned} \gamma_6^T(m, \varrho) = & \frac{1}{2^{\frac{7}{2}} \cdot 15\sqrt{\pi}} \int_0^1 d\tau \int_0^\infty dr r^2 \left[ \frac{1}{6} \mathbb{L}_{-\frac{3}{2}, -\frac{1}{2}} \varepsilon^{abc} G^{a\mu\nu} G^{b\mu\kappa} G^{c\nu\kappa} + \right. \\ & + \left( \frac{1}{2} \mathbb{L}_{-\frac{1}{2}, -\frac{3}{2}} - \frac{1}{16} \mathbb{L}_{-\frac{3}{2}, -\frac{1}{2}} \right) \left( (E^{ai;i})^2 + 2(B^{ai;4})^2 + \varepsilon^{abc} \varepsilon^{ijk} E^{ai} B^{bj} E^{ck} \right) - \\ & \left. - \left( \mathbb{L}_{\frac{1}{2}, -\frac{5}{2}} - \frac{5}{8} \mathbb{L}_{-\frac{1}{2}, -\frac{3}{2}} + \frac{1}{128} \mathbb{L}_{-\frac{3}{2}, -\frac{1}{2}} \right) (E^{ai;4})^2 \right]. \end{aligned} \quad (\text{B.14})$$

Figure 15 shows the strength of the trans-series corrections due to boundary conditions compared to the order-by-order large-mass expansion as well as the resulting large-mass restriction according to condition 3) in section 5.2.



(a) The leading heat kernel expansion shown in orange compared to 1.2 times the finite-temperature uncertainties depicted in blue (the factor 1.2 allows for a conservative restriction). The  $\varrho = 0.31$ -plane shows that for smaller caloron sizes the boundary condition - corrections are always smaller, while for  $\varrho \gtrsim 0.31$  a large enough quark mass is required.



(b) The minimal, i.e., lightest, possible heavy mass  $m_{\text{large, min, 3}}(\varrho)$  determined from [condition 3](#)). We choose it conservative so that  $\left| \frac{\gamma_6}{m^2} + \frac{\gamma_8}{m^4} + \frac{\gamma_{10}}{m^6} \right|$  exceeds  $\gamma_0^T + \gamma_4^T + \gamma_6^T$  by at least 20%. The blue lines mark data points and fill the area of allowed masses. We identify a roughly logarithmic growth of  $m_{\text{large, min, 3}}(\varrho)$ .

**Figure 15**

## C Diagonal Parts of the massless scalar Propagators

Here we show how to generalize the calculation of [section 4.2](#) to general (anti-)periodic scalar propagators  $\Delta^\pm(x, y, m = 0) = \Delta^\pm(x, y)$  using [\(4.3\)](#), [\(4.4\)](#) and [\(4.5\)](#). We show this for the traceful, i.e., diagonal parts. The traceless, off-diagonal parts can be obtained analogously by considering the terms  $\propto \vec{\sigma}$  in [\(4.5\)](#).

First, we calculate [\(4.5\)](#) for the general case, denoting  $\bar{t}_x - \bar{t}_y = \Delta\bar{t}$  and  $\bar{x} - \bar{y} = \bar{\Delta}$ :

$$\begin{aligned}
 F(\bar{x}, \bar{y}) &= \text{tr} \, 1 + \varrho^2 \sum_{k \in \mathbb{Z}} \frac{\vec{x} \cdot \vec{y} + (\bar{t}_x - k)(\bar{t}_y - k)}{\vec{x}^2 \vec{y}^2 + \vec{x}^2 (\bar{t}_y - k)^2 + \vec{y}^2 (\bar{t}_x - k)^2 + (\bar{t}_x - k)^2 (\bar{t}_y - k)^2} = \\
 &= 1 + \varrho^2 \text{Re} \left( \frac{i \vec{x} \cdot \vec{y} - |\vec{x}| (i |\vec{x}| + \Delta\bar{t})}{|\vec{x}| (\vec{y}^2 - (|\vec{x}| - i \Delta\bar{t})^2)} (\psi(-\bar{t}_x - i |\vec{x}|) - \psi(1 + \bar{t}_x + i |\vec{x}|)) \right) + (\bar{x} \leftrightarrow \bar{y}) =
 \end{aligned}$$

$$\begin{aligned}
&= 1 + \pi \varrho^2 \operatorname{Re} \left( \frac{i \vec{x} \cdot \vec{y} - |\vec{x}| (i |\vec{x}| + \Delta \bar{t})}{|\vec{x}| (|\vec{y}|^2 - (|\vec{x}| - i \Delta \bar{t})^2)} \cot(\pi(\bar{t}_x + i |\vec{x}|)) \right) + (\bar{x} \leftrightarrow \bar{y}) = \\
&= 1 + \frac{\pi \varrho^2}{c_1(|\vec{x}|, \bar{t}_x) d(|\vec{x}|, |\vec{y}|, \bar{t}_x, \bar{t}_y)} \left( -\Delta \bar{t} \bar{\Delta}^2 \sin(2\pi \bar{t}_x) + \right. \\
&\quad \left. + (|\vec{x}| \bar{\Delta}^2 + \hat{e}_{\vec{x}} \cdot \vec{y} \bar{\Delta}^2 + 2|\vec{x}| (\hat{e}_{\vec{x}} \cdot \vec{y})^2 - 2|\vec{x}| |\vec{y}|^2) \sinh(2\pi |\vec{x}|) \right) + (\bar{x} \leftrightarrow \bar{y}), \tag{C.1}
\end{aligned}$$

where  $\psi(z)$  is the digamma function, we used  $\psi(1-z) = \psi(z) + \pi \cot(\pi z)$  (reflection identity [61]) and shortened the notation by defining  $c_1(z_1, z_2) = \cosh(2\pi z_1) - \cos(2\pi z_2)$  as well as  $d(|\vec{x}|, |\vec{y}|, \bar{t}_x, \bar{t}_y) = ((|\vec{x}| - |\vec{y}|)^2 + \Delta \bar{t}^2)((|\vec{x}| + |\vec{y}|)^2 + \Delta \bar{t}^2)$ .

For calculating the periodic and anti-periodic propagators according to (4.3) and (4.4), we identify three types of time copy - summations in (C.1):

$$(1)^\pm = \sum_{j \in \mathbb{Z}} \frac{(\pm 1)^j}{4\pi^2 (\bar{\Delta} - j \hat{e}_4)^2}, \tag{C.2}$$

$$(2)_{x,y}^\pm = \sum_{j \in \mathbb{Z}} \frac{-(\pm 1)^j (\Delta \bar{t} - j)}{4\pi d(|\vec{x}|, |\vec{y}|, \bar{t}_x, \bar{t}_y + j)}, \tag{C.3}$$

$$(3)_{x,y}^\pm = \sum_{j \in \mathbb{Z}} \frac{(\pm 1)^j (|\vec{x}| (\bar{\Delta} - j \hat{e}_4)^2 + \hat{e}_{\vec{x}} \cdot \vec{y} (\bar{\Delta} - j \hat{e}_4)^2 + 2|\vec{x}| (\hat{e}_{\vec{x}} \cdot \vec{y})^2 - 2|\vec{x}| |\vec{y}|^2)}{4\pi (\bar{\Delta} - j \hat{e}_4)^2 d(|\vec{x}|, |\vec{y}|, \bar{t}_x, \bar{t}_y + j)}, \tag{C.4}$$

where  $(2)_{x,y}^\pm$  and  $(3)_{x,y}^\pm$  are not (explicitly)  $x \leftrightarrow y$ -symmetric and a factor of  $\pi$  has been absorbed into these terms. The full propagator then reads

$$\begin{aligned}
\Delta^\pm(x, y) = \operatorname{tr} \left[ (1)^\pm + \varrho^2 \left( (2)_{x,y}^\pm \frac{\sin(2\pi \tau_x)}{c_1(r_x, \tau_x)} + (2)_{y,x}^\pm \frac{\sin(2\pi \tau_y)}{c_1(r_y, \tau_y)} + \right. \right. \\
\left. \left. + (3)_{x,y}^\pm \frac{\sinh(2\pi r_x)}{c_1(r_x, \tau_x)} + (3)_{y,x}^\pm \frac{\sinh(2\pi r_y)}{c_1(r_y, \tau_y)} \right) \right] \frac{1}{\sqrt{\phi(x)\phi(y)}}. \tag{C.5}
\end{aligned}$$

Here we dropped the barred notation, because performing the  $j$ -summation describes the transition from  $\mathbb{R}^4$  to  $\mathbb{R}^3 \times S_{\text{rad}=1/2\pi}^1$ .

Explicitly, we find for the periodic case, denoting similarly to above  $\tau_x - \tau_y = \Delta\tau$ ,  $r_x - r_y = \Delta r$  and  $\vec{x} - \vec{y} = \vec{\Delta}$ :

$$(1)^+ = \frac{\sinh(2\pi |\vec{\Delta}|)}{4\pi |\vec{\Delta}| c_1(|\vec{\Delta}|, \Delta\tau)}, \tag{C.6}$$

$$(2)_{x,y}^+ = -\frac{\sinh(2\pi r_x) \sinh(2\pi r_y) \sin(2\pi \Delta\tau)}{8r_x r_y c_1(r_x + r_y, \Delta\tau) c_1(\Delta r, \Delta\tau)}, \tag{C.7}$$

$$(3)_{x,y}^+ = \frac{1}{16r_x} \left( \frac{\sinh(2\pi \Delta r)}{r_y c_1(\Delta r, \Delta\tau)} - \frac{\sinh(2\pi(r_x + r_y))}{r_y c_1(r_x + r_y, \Delta\tau)} + \frac{2 \sinh(2\pi |\vec{\Delta}|)}{|\vec{\Delta}| c_1(|\vec{\Delta}|, \Delta\tau)} \right). \tag{C.8}$$

Plugging our results (C.6) - (C.8) into (C.5) yields the traceful (diagonal) part of the full



massless, periodic propagator.<sup>11</sup>

For the anti-periodic propagator we proceed analogously. For numerical reasons, we split up the sum (3) $^-_{x,y}$  into three parts in doing so, (3.1) $^-_{x,y} = \sum_{j \in \mathbb{Z}} \frac{(-1)^j (|\vec{x}| + \hat{e}_{\vec{x}} \cdot \vec{y})}{4\pi d(|\vec{x}|, |\vec{y}|, \vec{t}_x, \vec{t}_y + j)}$ , (3.2) $^-_{x,y} = \sum_j \frac{(-1)^j |\vec{x}| (\hat{e}_{\vec{x}} \cdot \vec{y})^2}{2\pi(\Delta - j\hat{e}_4)^2 d(|\vec{x}|, |\vec{y}|, \vec{t}_x, \vec{t}_y + j)}$  and (3.3) $^-_{x,y} = -\sum_j \frac{(-1)^j |\vec{x}| \vec{y}^2}{2\pi(\Delta - j\hat{e}_4)^2 d(|\vec{x}|, |\vec{y}|, \vec{t}_x, \vec{t}_y + j)}$ . Also, we introduce the notation  $c_2(z_1, z_2) = \cosh^2(\pi z_1) - \cos^2(\pi z_2)$ :

$$(1)^- = \frac{\sinh(\pi|\vec{\Delta}|) \cos(\pi\Delta\tau)}{2\pi|\vec{\Delta}| c_1(|\vec{\Delta}|, \Delta\tau)}, \quad (\text{C.9})$$

$$(2)^-_{x,y} = -\frac{(\cosh(2\pi r_x) + \cosh(2\pi r_y) + \cos(2\pi\Delta\tau) + 1) \sinh(\pi r_x) \sinh(\pi r_y) \sin(\pi\Delta\tau)}{16r_x r_y c_2(r_x + r_y, \Delta\tau) c_2(\Delta r, \Delta\tau)}, \quad (\text{C.10})$$

$$(3)^-_{x,y} = -\left( \frac{(1 - \hat{e}_{\vec{x}} \cdot \hat{e}_{\vec{y}}) \sinh(\pi(r_x + r_y))}{(r_x + r_y) c_2(r_x + r_y, \Delta\tau)} + \frac{(1 + \hat{e}_{\vec{x}} \cdot \hat{e}_{\vec{y}}) \sinh(\pi\Delta r)}{\Delta r c_2(\Delta r, \Delta\tau)} - \frac{2 \sinh(\pi|\vec{\Delta}|)}{|\vec{\Delta}| c_2(|\vec{\Delta}|, \Delta\tau)} - (r_x + r_y \hat{e}_{\vec{x}} \cdot \hat{e}_{\vec{y}}) \left( \frac{\sinh(\pi(r_x + r_y))}{r_y(r_x + r_y) c_1(r_x + r_y, \Delta\tau)} + \frac{\sinh(\pi|\Delta r|)}{c_1(\Delta r, \Delta\tau)} \right) \right) \frac{\cos(\pi\Delta\tau)}{16r_x}. \quad (\text{C.11})$$

Using again (C.5) gives the massless, anti-periodic scalar propagator's diagonal part.<sup>12</sup>

<sup>11</sup>In the periodic propagator according to (C.5) we find one noteworthy simplification:

$$(2)^+_{x,y} \frac{\sin(2\pi\tau_x)}{c_1(r_x, \tau_x)} + (2)^+_{y,x} \frac{\sin(2\pi\tau_y)}{c_1(r_y, \tau_y)} = -\frac{(\cosh(2\pi r_x) \cos(2\pi\tau_y) + \cosh(2\pi r_y) \cos(2\pi\tau_x) - \sin(2\pi(\tau_x + \tau_y))) \sin(2\pi\Delta\tau) \sinh(2\pi r_x) \sinh(2\pi r_y)}{8r_x r_y c_1(r_x, \tau_x) c_1(r_y, \tau_y) c_1(r_x + r_y, \Delta\tau) c_1(\Delta r, \Delta\tau)}.$$

<sup>12</sup>We again give the one important simplification:

$$(2)^-_{x,y} \frac{\sin(2\pi\tau_x)}{c_1(r_x, \tau_x)} + (2)^-_{y,x} \frac{\sin(2\pi\tau_y)}{c_1(r_y, \tau_y)} = (\cosh(2\pi r_x) \sin(2\pi\tau_y) - \cosh(2\pi r_y) \sin(2\pi\tau_x) + \sin(2\pi\Delta\tau)) \times \frac{(\cosh(2\pi r_x) + \cosh(2\pi r_y) + \cos(2\pi\Delta\tau) + 1) \sinh(\pi r_x) \sinh(\pi r_y) \sin(\pi\Delta\tau)}{16r_x r_y c_1(r_x, \tau_x) c_1(r_y, \tau_y) c_2(r_x + r_y, \Delta\tau) c_2(\Delta r, \Delta\tau)}.$$

## References

- [1] A. A. Belavin, A. M. Polyakov, A. S. Schwarz and Y. S. Tyupkin, *Pseudoparticle solutions of the Yang-Mills equations*, *Physics Letters B* **59** (1975), no. 1 85–87.
- [2] B. J. Harrington and H. K. Shepard, *Euclidean solutions and finite temperature gauge theory*, *Nuclear Physics B* **124** (1977), no. 4 409–412.
- [3] J. I. Kapusta and C. Gale, *Finite-temperature field theory: Principles and applications*. Cambridge Monographs on Mathematical Physics. Cambridge University Press, 2011.
- [4] M. L. Bellac, *Thermal Field Theory*. Cambridge Monographs on Mathematical Physics. Cambridge University Press, 3, 2011.
- [5] D. J. Gross, R. D. Pisarski and L. G. Yaffe, *QCD and instantons at finite temperature*, *Rev. Mod. Phys.* **53** (1, 1981) 43–80.
- [6] J. Dragos, T. Luu, A. Shindler, J. de Vries and A. Yousif, *Confirming the existence of the strong CP problem in lattice QCD with the gradient flow*, *Phys. Rev. C* **103** (1, 2021) 015202.
- [7] C. Abel *et. al.*, *Measurement of the Permanent Electric Dipole Moment of the Neutron*, *Phys. Rev. Lett.* **124** (2, 2020) 081803.
- [8] S. Weinberg, *A New Light Boson?*, *Phys. Rev. Lett.* **40** (1, 1978) 223–226.
- [9] F. A. Wilczek, *Problem of Strong P and T Invariance in the Presence of Instantons*, *Phys. Rev. Lett.* **40** (1, 1978) 279–282.
- [10] R. D. Peccei and H. R. A. Quinn, *CP Conservation in the Presence of Instantons*, *Phys. Rev. Lett.* **38** (1977) 1440–1443.
- [11] R. D. Peccei and H. R. A. Quinn, *Constraints Imposed by CP Conservation in the Presence of Instantons*, *Phys. Rev. D* **16** (1977) 1791–1797.
- [12] F. Chadha-Day, J. Ellis and D. J. E. Marsh, *Axion dark matter: What is it and why now?*, *Science Advances* **8** (2, 2022) eabj3618.
- [13] G. G. di Cortona, E. Hardy, J. P. Vega and G. Villadoro, *The QCD axion, precisely*, *Journal of High Energy Physics* **2016** (1, 2016) 34.
- [14] D. J. E. Marsh, *Axion cosmology*, *Physics Reports* **643** (7, 2016) 1–79.
- [15] I. G. Irastorza, *An introduction to axions and their detection*, *SciPost Phys. Lect. Notes* (2022) 45.
- [16] M. Kuster, G. Raffelt and B. Beltrán, eds., *Axions. Theory, Cosmology and Experimental Searches*, vol. 741. Springer, 2008.
- [17] L. Di Luzio, M. Giannotti, E. Nardi and L. Visinelli, *The landscape of QCD axion models*, *Physics Reports* **870** (2020) 1–117. The landscape of QCD axion models.
- [18] O. Wantz and E. P. S. Shellard, *Axion cosmology revisited*, *Phys. Rev. D* **82** (12, 2010) 123508.
- [19] S. Borsányi, M. Dierigl, Z. Fodor, S. D. Katz, S. W. Mages, D. Nogradi, J. Redondo, A. Ringwald and K. K. Szabó, *Axion cosmology, lattice QCD and the dilute instanton gas*, *Physics Letters B* **752** (2016) 175–181.
- [20] M. Gorghetto and G. Villadoro, *Topological susceptibility and QCD axion mass: QED and NNLO corrections*, *Journal of High Energy Physics* **2019** (3, 2019) 33.

- [21] Z.-Y. Lu, M.-L. Du, F.-K. Guo, U.-G. Meißner and T. Vonk, *QCD  $\theta$ -vacuum energy and axion properties*, *Journal of High Energy Physics* **2020** (May, 2020) 1.
- [22] S. Borsányi *et. al.*, *Calculation of the axion mass based on high-temperature lattice quantum chromodynamics*, *Nature* **539** (2016), no. 7627 69–71.
- [23] S. Borsányi, Z. Fodor, C. Hoelbling, S. D. Katz, S. Krieg and K. K. Szabo, *Full result for the QCD equation of state with 2+1 flavors*, *Phys. Lett. B* **730** (2014) 99–104 [[1309.5258](#)].
- [24] **HotQCD** Collaboration, A. Bazavov *et. al.*, *Equation of state in ( 2+1 )-flavor QCD*, *Phys. Rev. D* **90** (2014) 094503 [[1407.6387](#)].
- [25] V. B. Klaer and G. D. Moore, *The dark-matter axion mass*, *Journal of Cosmology and Astroparticle Physics* **2017** (Nov, 2017) 049.
- [26] B. J. Harrington and H. K. Shepard, *Periodic Euclidean solutions and the finite-temperature Yang-Mills gas*, *Phys. Rev. D* **17** (4, 1978) 2122–2125.
- [27] P. T. Jahn, G. D. Moore and D. Robaina,  $\chi_{top}(T \gg T_c)$  in pure-gluon QCD through reweighting, *Phys. Rev. D* **98** (2018), no. 5 054512 [[1806.01162](#)].
- [28] P. T. Jahn, G. D. Moore and D. Robaina, *Improved Reweighting for QCD Topology at High Temperature*, [2002.01153](#).
- [29] **Particle Data Group** Collaboration, R. L. Workman *et. al.*, *Review of Particle Physics*, *PTEP* **2022** (2022) 083C01.
- [30] G. 't Hooft, *Computation of the quantum effects due to a four-dimensional pseudoparticle*, *Phys. Rev. D* **14** (12, 1976) 3432–3450.
- [31] G. 't Hooft, *Erratum: Computation of the quantum effects due to a four-dimensional pseudoparticle*, *Phys. Rev. D* **18** (9, 1978) 2199–2200.
- [32] R. Bott, *An Application of Morse theory to the topology of Lie groups*, *Bull. Soc. Math. Fr.* **84** (1956) 251–281.
- [33] C. Bernard, *Gauge zero modes, instanton determinants, and quantum-chromodynamic calculations*, *Phys. Rev. D* **19** (5, 1979) 3013–3019.
- [34] S. Vandoren and P. van Nieuwenhuizen, *Lectures on instantons*, 2008.
- [35] C. G. Callan, R. Dashen and D. J. Gross, *Toward a theory of the strong interactions*, *Phys. Rev. D* **17** (5, 1978) 2717–2763.
- [36] L. S. Brown, R. D. Carlitz, D. B. Creamer and C. Lee, *Propagation functions in pseudoparticle fields*, *Phys. Rev. D* **17** (3, 1978) 1583–1597.
- [37] L. S. Brown and C. Lee, *Massive propagators in instanton fields*, *Phys. Rev. D* **18** (9, 1978) 2180–2183.
- [38] M. F. Atiyah, N. J. Hitchin, V. G. Drinfeld and Y. I. Manin, *Construction of instantons*, *Physics Letters A* **65** (1978), no. 3 185–187.
- [39] C. Bernard, *Instanton interactions at the one-loop level*, *Phys. Rev. D* **18** (9, 1978) 2026–2041.
- [40] F. Rennecke, *Higher topological charge and the QCD vacuum*, *Phys. Rev. Res.* **2** (9, 2020) 033359.
- [41] O.-K. Kwon, C. Lee and H. Min, *Massive field contributions to the QCD vacuum tunneling amplitude*, *Phys. Rev. D* **62** (11, 2000) 114022.

- [42] G. V. Dunne, J. Hur, C. Lee and H. Min, *Calculation of QCD instanton determinant with arbitrary mass*, *Phys. Rev. D* **71** (4, 2005) 085019.
- [43] J. Ghiglieri, A. Kurkela, M. Strickland and A. Vuorinen, *Perturbative thermal QCD: Formalism and applications*, *Physics Reports* **880** (2020) 1–73. Perturbative Thermal QCD: Formalism and Applications.
- [44] I. Ojima, *Lorentz Invariance Versus Temperature in QFT*, *Lett. Math. Phys.* **11** (1986) 73.
- [45] D. A. Kirzhnits and A. D. Linde, *Symmetry Behavior in Gauge Theories*, *Annals Phys.* **101** (1976) 195–238.
- [46] C. Lee, H. W. Lee and P. Pac, *Calculation of one-loop instanton determinants using propagators with space-time dependent mass*, *Nuclear Physics B* **201** (1982), no. 3 429–460.
- [47] B. S. DeWitt, *Quantum field theory in curved spacetime*, *Physics Reports* **19** (1975), no. 6 295–357.
- [48] D. V. Vassilevich, *Heat kernel expansion: user’s manual*, *Physics Reports* **388** (2003), no. 5 279–360.
- [49] E. Megías, E. Ruiz Arriola and L. L. Salcedo, *Thermal heat kernel expansion and the one-loop effective action of QCD at finite temperature*, *Phys. Rev. D* **69** (6, 2004) 116003.
- [50] E. Megías, E. Ruiz Arriola and L. L. Salcedo, *The Polyakov loop and the heat kernel expansion at finite temperature*, *Physics Letters B* **563** (2003), no. 3 173–178.
- [51] D. Fliegner, P. Haberl, M. G. Schmidt and C. Schubert, *The Higher Derivative Expansion of the Effective Action by the String Inspired Method, II*, *Annals of Physics* **264** (1998), no. 1 51–74.
- [52] D. Fliegner, P. Haberl, M. G. Schmidt and C. Schubert, *The Higher derivative expansion of the effective action by the string inspired method. Part 2*, 1998.
- [53] B. Shoshany, *OGRe: An Object-Oriented General Relativity Package for Mathematica*, *Journal of Open Source Software* **6** (2021), no. 65 3416.
- [54] S. G. Johnson, “Multi-dimensional adaptive integration in C: The Cubature package.” <https://github.com/stevengj/cubature>, 2005.
- [55] A. C. Genz and A. A. Malik, *Remarks on algorithm 006: An adaptive algorithm for numerical integration over an N-dimensional rectangular region*, *Journal of Computational and Applied Mathematics* **6** (1980) 295–302.
- [56] J. Berntsen, T. O. Espelid and A. Genz, *An adaptive algorithm for the approximate calculation of multiple integrals*, *ACM Transactions on Mathematical Software* **17** (1991) 437–451.
- [57] J. M. Bull and T. L. Freeman, *Parallel globally adaptive algorithms for multi-dimensional integration*, *Applied Numerical Mathematics* **19** (1995) 3–16.
- [58] K. Fukushima and V. Skokov, *Polyakov loop modeling for hot QCD*, *Progress in Particle and Nuclear Physics* **96** (2017) 154–199.
- [59] A. Meurer *et. al.*, *SymPy: symbolic computing in Python*, *PeerJ Computer Science* **3** (Jan., 2017) e103.
- [60] The mpmath development team, *mpmath: a Python library for arbitrary-precision floating-point arithmetic (version 1.3.0)*, 2023. <https://mpmath.org/>.

- [61] M. Abramowitz and I. Stegun, *Handbook of Mathematical Functions with Formulas, Graphs, and Mathematical Tables*. Selected government publications. New York, 10th print, with corr. ed., 1972.